Upper Cretaceous-Paleogene Stratigraphy and Development of the Mìmir High, Vøring Transform Margin, Norwegian Sea

Stéphane Polteau[1,2,3*], Sverre Planke[1,4], Dmitry Zastrozhnov[1], Mohamed Mansour Abdelmalak[1,4], Nina Lebedeva-Ivanova[1], Ellen Eckhoff Planke[1], Henrik Hovland Svensen[4], Adriano Mazzini[4], Laurent Gernigon[5], Reidun Myklebust[6], Bent Erlend Kjølhamar[6], Rolf Birger Pedersen[7], Nils Rune Sandstå[8], Stefan Bünz[9]

[1]Volcanic Basin Petroleum Research, Oslo, Norway

[2]Institute for Energy Technology, Kjeller, Norway

[3]SurfExGeo, Oslo, Norway

[4]Centre for Earth Evolution and Dynamics, University of Oslo, Norway

[5]Norges Geologisk Undersøkelse (NGU), Trondheim, Norway

[6]TGS, Asker, Norway

[7]K.G. Jebsen Centre for Deep Sea Research, Department of Earth Science, University of Bergen, Norway

[8]Norwegian Petroleum Directorate, Stavanger, Norway

[9]Center for Arctic Gas Hydrate, Environment and Climate, The Arctic University of Norway, Norway

**corresponding author*

ABSTRACT

Transform margins represent strike-slip type of plate boundaries that form during continental breakup and initial ocean opening. They are often characterized by margin-parallel highs with exposed pre- and syn-rift sequences. The Vøring Transform Margin, offshore mid-Norway, initiated in the earliest Eocene during the opening of the NE Atlantic. Here, 2D seismic reflection data reveal a transform margin high, the Mímir High. The western flank of this undrilled structure is a kilometer-high escarpment where seismic reflections of pre-breakup age are truncated at the seafloor. The aim of this study was to recover seabed rock samples from the outcropping or shallowly buried sedimentary sequences to provide a geological tie to the regional seismic framework, thereby constraining the basin history and tectono-stratigraphic development. Seabed samples were successfully collected from 14 gravity core and Selcore stations and 10 ROV (remotely operated vehicle) sites along a 750 m high sampling profile, recovering clay, shales, sandstones and glacial dropstones. Biostratigraphy results revealed that the ages of the sedimentary rocks follow the correct stratigraphic order predicted by the initial seismic interpretation, with Upper Cretaceous sediments at the base and early Eocene sediments at the top. The integrated interpretation shows that the Mìmir High area, including parts of the outer Vøring and Møre basins and the proto-Jan Mayen Microplate Complex, were characterized by the deposition of late Campanian to early Maastrichtian, near coastal and shale-dominated sequences with poor source rock qualities. The early Paleocene samples indicate deep marine conditions that abruptly ended by rapid uplift of the Mìmir High in the earliest Eocene. Finally, a reworked Pliensbachian palynomorph assemblage in potential early Eocene strata indicate the presence of exposed Mesozoic sequences in the vicinity of the Mìmir High. We argue that some of the early Eocene sediments where deposited within a hypothetical drainage system sourced from Greenland (Traill Ø or

Jameson Land) and/or from the Jan Mayen Ridge prior to continental separation, and not the result of recent ice-rafting.

Keywords: Vøring Transform Margin, NE Atlantic, Seafloor Sampling, Upper Cretaceous, Paleogene

INTRODUCTION

Transform, oblique, and extensional margins are the three types of plate boundaries that form during continental breakup and ocean opening. Transform margins and sheared margins in general represent 16% of the cumulated length of the world's continental margins (Mercier de Lépinay et al., 2016), and are not as well studied as divergent or convergent continental margins (e.g., Nemčok et al., 2016). Generally, transform margins display a narrow and steep continental slope underlain by a very sharp crustal necking zone close to the continent-ocean boundary (e.g., Antobreh et al., 2009; Basile, 2015; Loncke et al., 2020; Mercier de Lépinay et al., 2016; Turner et al., 2003). Transform margins are often characterized by elevated marginal highs along the continental slope (**Fig. 1**), whose steepness may prevent any significant sediment deposition but instead favor gravity-driven collapses at different scales (e.g., Loncke and Maillard, 2015; Pattier et al., 2013). Consequently, the erosion of the steep continental slope may locally cause the deep parts of the pre and syn-rift sedimentary sequences as well as the continental basement to crop out at the seafloor (**Fig. 1.B**). Lateral heat transport from the nascent oceanic to the adjacent continental lithosphere could generate melt accumulation at the base of the lower crust to form dense lower crustal bodies. Such magmatic bodies can contribute to the regional uplift of the marginal plateau (Antobreh et al., 2009) (**Fig. 1**), but often appear to be local along transform margins (Berndt et al., 2001). Several mechanisms have been proposed to explain local uplift along the transform margin: differential thermal subsidence, lateral heat transfer, extension perpendicular to the transform or erosion of a lithospheric plate along the transform boundary (Basile and Allemand, 2002).

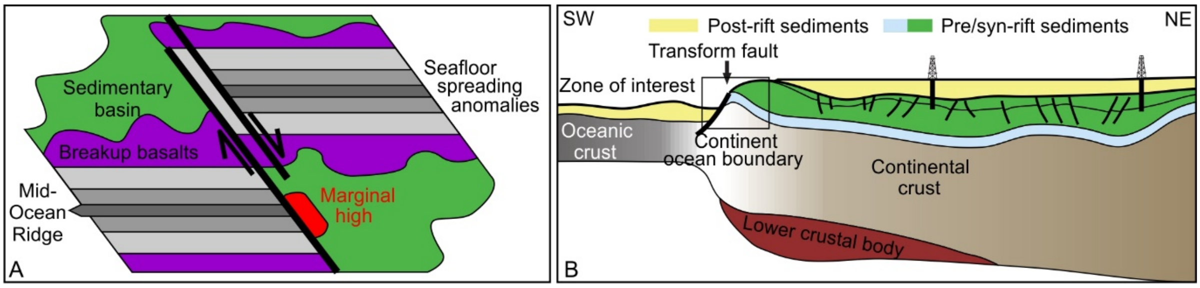

***Fig. 1**. Schematic representation of a typical transform margin (after Berndt et al., 2001): **A** in a map view showing that the uplift of the marginal high may be related to the Mid-Ocean Ridge during early phase of breakup, and **B** in a profile across a transform margin showing the presence of outcropping pre-breakup age sequences on the uplifted marginal high, which is our zone of interest.*

On volcanic rifted margins, thick breakup-related basalt successions commonly cover the sedimentary sequences expected to outcrop along the continent-ocean transition (Fig. 1.A; e.g., Abdelmalak et al., 2016a). These sedimentary sequences are sometimes poorly mapped due to difficulties with sub-basalt seismic imaging and limited borehole control. Prominent transform margins are located along the southern Exmouth Plateau offshore Western Australia (Lorenzo et al., 1991; Lorenzo and Vera, 1992), the continental margin off the Ivory Coast and Ghana (Mascle et al., 1998), the western Barents Sea margin including the Vestbakken Volcanic Province (Faleide et al., 1988), and the Vøring Transform Margin offshore Norway (Berndt et al., 2001). Due to the specific tectono-magmatic conditions of transform margin (Berndt et al., 2001), magmatism is often reduced along the transform segments of volcanic margin system and the volcanic deposits may be locally absent, hence providing windows for seismic investigations and potential drilling of pre-breakup sequences. This is the case of a restricted segment of the Vøring Transform Margin, formed during the opening of the NE Atlantic about 55 Ma ago (**Fig. 2A-C**) (e.g.: Abdelmalak et al., 2016a; Abdelmalak et al., 2016b; Berndt et al., 2000). Here, 2D seismic reflection data image the Mímir High, an uplifted transform margin high showing truncated reflections along the slope of the transform margin

(**Fig. 3**). Thanks to its specific geological setting, the Mímir High provides a unique opportunity to recover *in situ* rock fragments from outcrops at the seabed. Such data are crucial to calibrate and document the stratigraphy and to understand the tectono-magmatic development of the Vøring Transform Margin prior to, during and after continental breakup.

In this contribution, we combine and present the results from seabed sampling of the Mímir High acquired during the Vøring Transform Margin Sampling (VTMS00) and NPD 2013-B surveys carried out in 2000 and 2013, respectively (**Figs. 2** and **3**). During the VTMS00 cruise, we used gravity corer and a Selcorer to recover near *in situ* rock fragments and thin overburden sediments. The 2013-B cruise used a ROV (remotely operated vehicle) to recover outcrop material in the same area. The samples were subsequently analyzed and dated using conventional sedimentology, organic geochemistry and biostratigraphy. In such a frontier area, the results provide a crucial tie to the Upper Cretaceous and Paleogene sequences imaged by the seismic data.

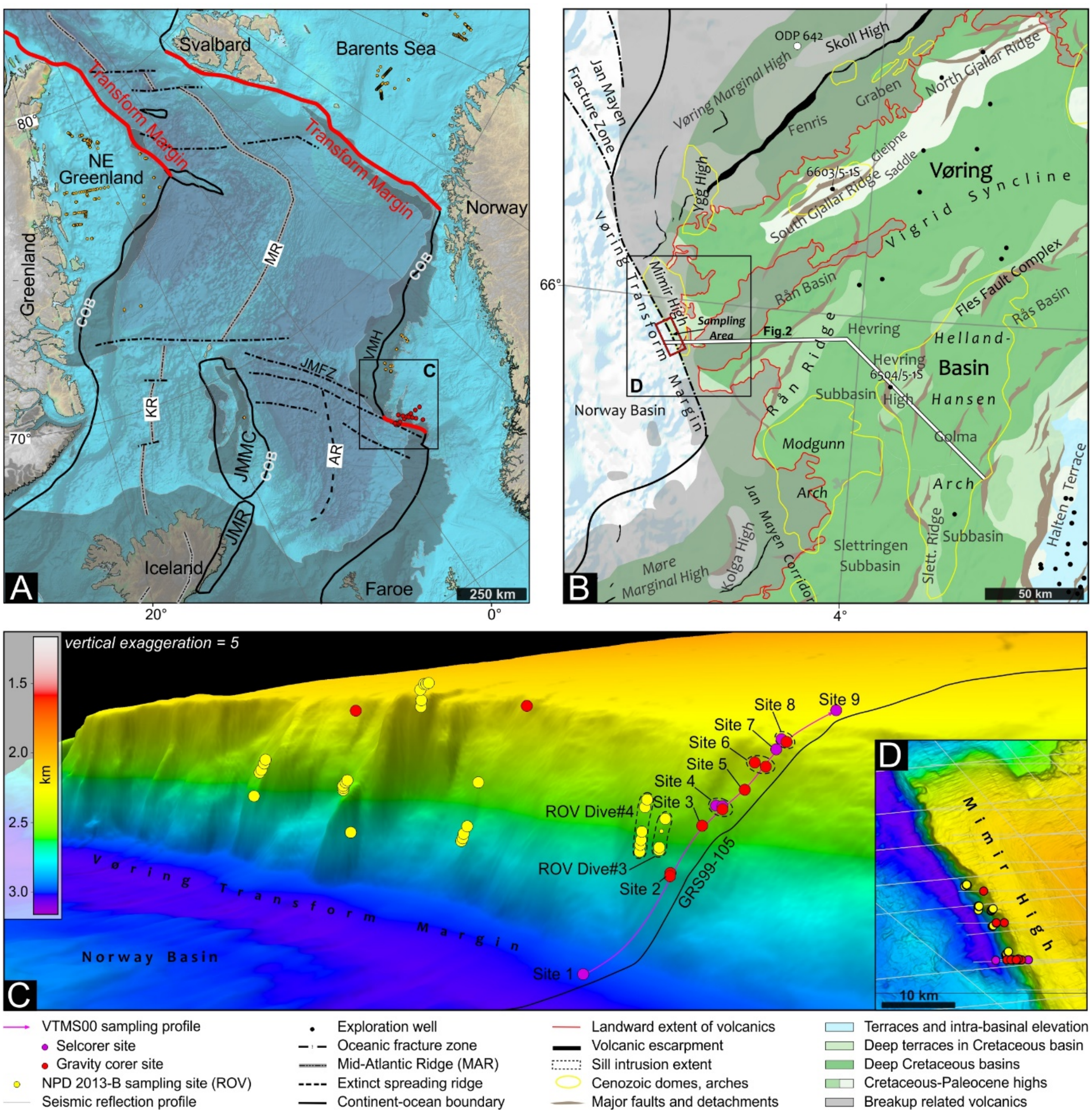

***Fig. 2**. Regional setting and seafloor sampling profile. **A**. Regional setting showing onshore and offshore distribution of breakup-related volcanic rocks (grey shade) in the NE Atlantic (modified after Abdelmalak et al., 2017; Gernigon et al., 2019). The map shows the location of the VTMS00 (Vøring Transform Margin Sampling 2000) and additional VBPR/TGS sampling sites in the NE Atlantic (yellow dots). **B**. Nomenclature map (modified after Zastrozhnov et al., 2020) showing sampling sites, scientific wells and the location of the well 6504/5-1S (Gemini) along a regional seismic profile (**Fig. 3**). **C** and **D**. High-resolution multi-beam bathymetry showing a 3D and map view with the location of 2D seismic lines and sampling sites of the survey area. AR: Aegir Ridge; COB: continent ocean boundary; JMMC: Jan Mayen Microplate Complex; JMR: Jan Mayen Ridge; KR: Kolbeinsey Ridge; MR: Mohn's Ridge; VMH: Vøring Marginal High. Bathymetric data courtesy of NPD.*

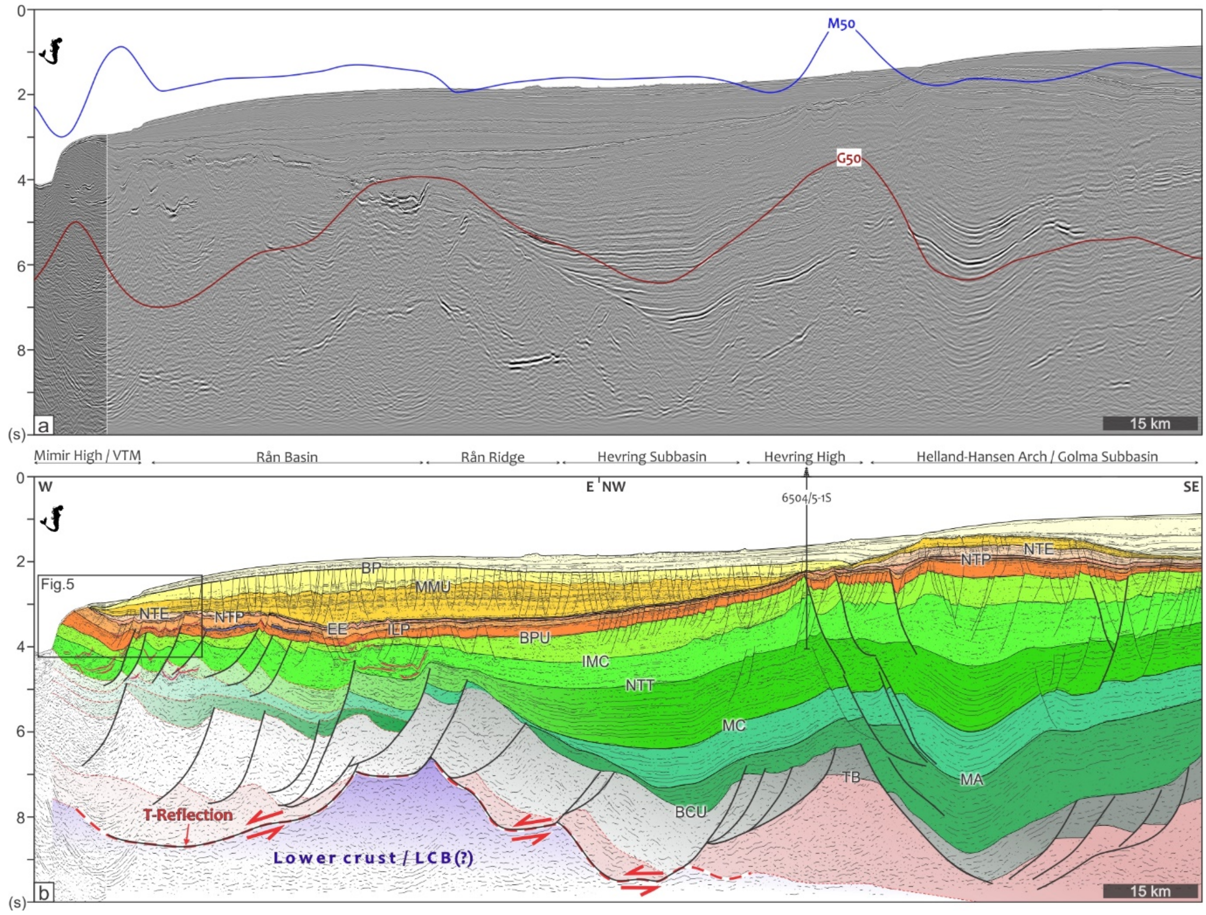

Fig. 3. *Regional un-interpreted (**a**) and interpreted (**b**) composite seismic profile with 50-km high-pass filtered Bouguer (G50, red curve) and magnetic (M50, blue curve) potential field anomalies. The ages of the regional Cretaceous and younger horizons were tied to well 6504/5-1S (Gemini) ca. 100 km away from the Mìmir High (see **Fig. 1.B**). Horizons correspond to: LCB (Lower Crustal Body), TB (Top Basement), BCU (Base Cretaceous Unconformity), MA (Mid-Albian), MC (Mid-Cenomanian), NTT (Near Top Turonian), IMC (Intra-Mid-Campanian), BPU (Base Paleogene Unconformity), ILP (Intra-Late Paleocene), NTP (Near Top Paleocene, EE (Early Eocene), NTE (Near Top Eocene), MMU (Mid-Miocene Unconformity), BP (Base Pleistocene). Data courtesy of TGS.*

Geological setting

The conjugate volcanic rifted margins along the NE Atlantic are part of the North Atlantic Igneous Province, and were formed during the final fragmentation of Pangea in the early Cenozoic (Ganerød et al., 2010; Gernigon et al., 2019; Hansen et al., 2009; Meyer et al., 2007; Saunders et al., 1997; Skogseid and Eldholm, 1987; Talwani and Eldholm, 1977; Torsvik et al., 2001). On the mid-Norwegian margin, the onset of continental breakup marked a culmination of a ~350 Ma long period of predominantly extensional deformation (Doré et al., 1999b; Skogseid et al., 2000; Tsikalas et al., 2008; Ziegler, 1988), including the late Paleozoic-Triassic, Upper Jurassic - Lower to mid-Cretaceous, and Upper Cretaceous-Paleocene rifting episodes (Blystad et al., 1995; Brekke, 2000; Doré et al., 1999a; Faleide et al., 2008; Gernigon et al., 2019; Gernigon et al., 2004; Tsikalas et al., 2012). Severe Upper Jurassic - Lower to mid-Cretaceous lithospheric extension and normal faulting episodes resulted in the formation of large sag-type sedimentary basins observed at present day in the Vøring and Møre basins (Blystad et al., 1995; Brekke, 2000; Gernigon et al., 2019; Lundin and Doré, 1997; Mjelde et al., 2008; Zastrozhnov et al., 2020). Here, up to 10-12 km of Cretaceous-Cenozoic sediments accumulated in the main depocenters (Blystad et al., 1995; Brekke, 2000; Lien et al., 2006; Zastrozhnov et al., 2018).

During the Upper Cretaceous–Paleocene, the locus of maximum extension migrated and/or jumped NW toward the outer part of the mid-Norwegian margin (Skogseid et al., 2000; Zastrozhnov et al., 2020). This rifting episode eventually led to a diachronous and propagating continental breakup during Paleocene- early Eocene (Gernigon et al., 2019). Aeromagnetic data suggest that the spreading and magmatic activity possibly initiated about 1-2 Ma earlier in the Møre and Jan Mayen Corridor segments when compared to the rest of the Vøring Margin (Gernigon et al., 2019; Zastrozhnov et al., 2020). The massive, transient, and breakup-related magmatic activity along the continental-oceanic transition resulted in the emplacement of several kilometer thick subaerial and subaqueous extrusive volcanic sequences (Eldholm et al., 2000; Eldholm and Grue, 1994). Synchronous intrusive complex and associated hydrovolcanic vents were emplaced within the adjacent sedimentary basins (Planke et al., 2005). Due to specific tectonic and lithospheric settings of the Vøring Transform

Margin, Berndt et al. (2001) showed that the magmatic activity was locally reduced in the vicinity of the Jan Mayen Fracture Zone compared to the adjacent Møre and Vøring marginal highs.

The pre-breakup structural development of the Vøring Transform Margin is poorly constrained, but is traditionally interpreted to be a by-product directly or indirectly related to the presence of the Jan Mayen Lineament or the Jan Mayen Corridor that represents and old rift-related transfer zone system possibly linked with older basement inherited structures (Brekke, 2000; Gernigon et al., 2014). The first major strike-slip movements along the paleo-Vøring Transform Margin most likely initiated in the Maastrichtian (Brekke, 2000), but the uplift of the Mìmir High initiated at the early breakup stage in the late Paleocene - earliest Eocene (Berndt, 2000). The post-breakup Cenozoic activity of the transform margin could be related to the strain partitioning along the Jan Mayen Lineament due to kinematic changes in the adjacent NE Atlantic spreading system (Doré et al., 2008).

In the outer Vøring Basin, the deepest borehole 6603/5-1S (Dalsnuten well located on the South Gjallar Ridge; see **Fig. 2B**) reached the Lower Cretaceous Lange Formation, and hence the older sedimentary successions remain unconstrained. However, the Dalsnuten well is not fully suitable for a regional seismic tie due to its position on a structural high affected by complex faulting and controversial biostratigraphy (Zastrozhnov et al., 2020). Alternatively, well 6504/5-1S (Gemini) drilled in the center of the Vøring Basin can be used for a seismic tie (**Fig. 2B**). The Gemini well is located more than 100 km away from the sampling profile, and thus provides only regional and relative age constraints of the Mìmir High geology, down to Upper Cretaceous. Indeed, the identification of deep pre-Cretaceous and deep Cretaceous sequences along the distal and outer mid-Norwegian margin mostly relies on the geophysical interpretation of potential field data (Zastrozhnov et al., 2018), seismic refraction data (Kvarven et al., 2016; Mjelde et al., 2009; Mjelde et al., 2005; Raum et al., 2002), and seismic reflection data (Gernigon et al., 2003; Péron-Pinvidic and Osmundsen, 2016; Zastrozhnov et al., 2020). In this context, the Mímir High provides a unique opportunity to ground truth the geology in the outer Vøring Basin.

METHODS

Sampling equipment and strategy

Sampling operations during the VTMS00 cruise were carried out using the R/V Håkon Mosby, a research vessel operated by the University of Bergen. Sampling operations during the 2013-B survey were carried out onboard the M/V Seabed Worker, a multi-purpose subsea vessel operated by Swire Seabed. VTMS00 sampling stations were located along seismic line GRS99-105 at water depths ranging from 2000 to 3000 m. We sampled the seabed of the Mìmir High using a gravity corer (GC), a Selcorer (SC), a dredge (results not reported here) and a ROV (Remotly Operated Vehicle). The gravity coring system consisted of a lead weight of 800 kg attached to a six or three-meter-long core barrel (**Fig. 4**). The gravity corer was dropped in freefall from 50 m above the seafloor to maximize penetration into the sediment. The Selcorer is similar to the gravity corer, but includes a hydrostatic motor utilizing the difference in pressure between the surface and sea bottom to increase penetration (Kristoffersen et al., 2006). The Selcorer was dropped on the seafloor, and the core is hammered either until it reached full penetration of the 12-meter barrel or until the energy available for the motor is exhausted. A transponder was attached to the Selcorer, and the corer was located 20 to 90 m SW of the vessel. The ROV was a Schilling HD28 model equipped with a manipulator paired with a modified industrial chain saw and a drawer to store the samples.

The sampling strategy was to recover truncated seismic strata at or below the seafloor. A steep slope angle will favor hard substrate to remain exposed at the seafloor, while flat areas allow well-developed alteration profiles overlaid by overburden sediments (**Fig. 4**). Differentiating outcrops from recent overburden sediments at the seabed is rather straightforward when using a ROV. The live video feed provides direct visual observations that can be used to discriminate horizontal to sub-horizontal layered sedimentary strata truncated at the seabed from monotonous muddy seafloor representing the recent overburden sediments blanketing the outcrops. Nevertheless, large slide blocks may exist on steep escarpment, but could be difficult to distinguish from solid outcrops even with ROV video.

Gravity cores can sample rock fragments buried by several meters of overburden sediments (**Fig. 4**). The assignation of overburden versus near in situ subcrop is based on the lithology together with the palynology assemblages of the recovered material. Overburden material mostly consists of unconsolidated and water-saturated sediments dominated by recent palynomorph assemblages of the Quaternary age. Subcropping sequences are interpreted to be present when well to poorly lithified rock fragments of the same lithology and biostratigraphic assemblage were recovered in the bit and core catcher. However, identifying subcropping sequences close to the seafloor may not be trivial, since the recovery may consist of soft clay resulting from extreme weathering-like alteration of the subcrop. The palynology assemblages of the overburden clays and altered subcrops are markedly different, with the latter characterizing one specific pre-Quaternary stratigraphic interval (Polteau et al., 2019). Hence, the confidence in identifying an in situ subcrop is high when only rock fragments have been sampled, while altered subcrops can sometimes only be identified by a palynomorph assemblage and organic facies specific to a narrow and well-documented regional stratigraphic interval. In addition, we commonly observe contamination of recent forms in subcrop material, which is mostly related to mixing along the liner walls during penetration in the seafloor of the corer.

The Selcore and gravity core handling procedures were identical. First, the bit and the core catcher were removed from the core barrel and brought to the laboratory to describe and sample their contents. The liner was then removed from the casing, cut into 1 m sections on deck, and caps were placed at both ends. The sections were then carried to the laboratory where the section tops were described and sampled for analyses. The liners containing lithified to semi-lithified material were split onboard, logged, photographed, sampled for analyses, labelled and sealed.

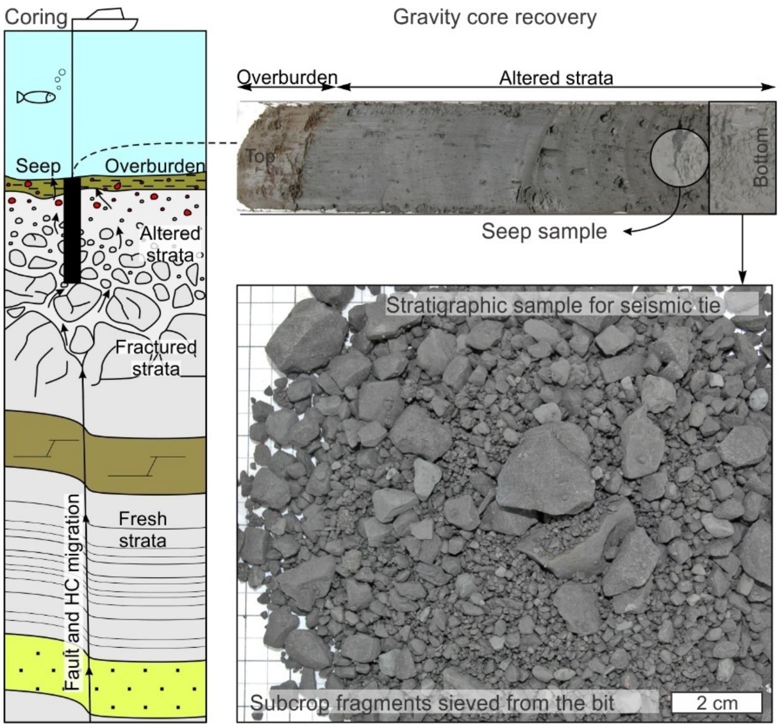

Fig. 4. *Sketch showing the gravity coring method, including alteration of the subcropping strata which are decreasing with depth. There is an increase in dilution of in situ lithologies by recent overburden sediments (clay, sand and dropstones in red) towards the seafloor. The figure is mainly based on observations from this study and sampling surveys on the southern Jan Mayen Ridge (Polteau et al., 2019) and in the Baffin Bay (Abdelmalak et al., 2019). Scale is approximate.*

Biostratigraphy

Biostratigraphic analyses were carried out at Stratlab (now Applied Petroleum Technology, APT), and included 24 samples for palynology and 13 samples for a qualitative micropaleontological assessment. Sediment samples were initially screened for palynological analysis during the cruise, and subsequently re-analyzed onshore for a more reliable biostratigraphic interpretation. Additional biostratigraphic analysis were carried out by Ichron and NPD on six samples collected during the ROV survey.

The identification of palynomorphs was done using a binocular microscope. The palynological analyses were quantitative and based on a minimum of 200 pollen counts when possible. A general description of the kerogen composition for each sample included measurements of the thermal alteration values following a modified Thermal Alteration Index (TAI). TAI values were determined based on assessments of resistant organic material in the samples consisting of pollen/spores, dinoflagellate cysts, and other algae and kerogen particles. The later were considered to interpret the various depositional environments. The sediment fraction larger than 63 μm was kept for micropaleontological analysis. A semi-quantitative assessment of each recorded taxon was carried out using a Wild M7 stereomicroscope.

Organic geochemistry

Eleven selected sedimentary rock fragments from the VTMS00 survey were analyzed at the APT laboratory for Total Organic Carbon (TOC) content (wt.%) and Rock-Eval pyrolysis using a Rock-Eval 6 instrument which provides hydrocarbon (HC) source characteristics (Espitalié et al., 1986). The technique uses temperature programmed heating of a small amount of rock (100 mg) in an inert atmosphere (helium or nitrogen) to determine the quantity of free hydrocarbons present in the sample (S1 peak), and the amount of hydrocarbons and compounds containing oxygen (CO_2) that are produced during the thermal cracking of the insoluble organic matter (kerogen) in the rock (S2 and S3 peaks respectively) (Lafarge et al., 1998). The maturity levels of kerogen in the samples are defined by the Hydrogen Index (HI, mg HC/g TOC), the Oxygen Index (OI, mg CO2/g TOC), and a Tmax (expressed in °C). HI is the ratio between S2 and the TOC; OI is the ratio between S3 and the TOC; and Tmax is the temperature at maximum pyrolytic hydrocarbon generation that varies as a function of the natural thermal maturity of the organic matter (Lafarge et al., 1998).

Six of the Mìmir High samples were selected for vitrinite reflectance measurements following the standard procedures described in NIGOGA (Norwegian Industry Guide to Organic Geochemical Analysis) using the methodology described in Weiss et al. (2000). Vitrinite reflectance measurements were done with a Zeiss Universal MPM03 photometer microscope. The analysis was performed on kerogen concentrates prepared following the kerogen isolation procedures outlined in Weiss et al. (2000).

Seismic data and interpretation

The seismic database of the Mìmir High consists of regional conventional 2D lines and high resolution 2D profile tying the sampling sites. Seismic line GRS99-105 was acquired in 1998 by TGS using a 6 km long streamer and a 3800 in^3 airgun array shooting every 37.5 m. Regional MNR lines were acquired in 2004-2011 using a 10 km long streamer and a 4640 in^3 airgun array shooting every 25 m. The high resolution 2D seismic line was collected across VTMS00 sampling sites in August 2020 by UiT The Arctic University of Norway using a 200 m long streamer and two mini (45 in^3) GI airguns shooting every 10 s (12-15 m). The GRS99 and MNR lines were conventionally processed and migrated on 6.25-12.5 m bin size with a dominant spectrum in the 10-40 Hz and 10-60 Hz ranges, respectively. The high resolution 2D seismic was fast track processed and migrated on 6.25 m bin size to preserve a useful signal between 40 and 260 Hz.

During the study, we interpreted seismic horizons along a regional seismic tie line from the Gemini well (6504/5-1S) to the sampling profile on the Mìmir High ca. 100 km away using a composite line including the vintage GRS99-105 profile across the Mìmir High, combined with more recent regional MNR 2D lines (**Fig. 3**). We use the regional and revised stratigraphic framework from Zastrozhnov et al. (2020) as reference for the pre-Eocene sequences, whereas Eocene-Pleistocene horizons were picked along the composite line. The interpretation of the seismic data across the Mìmir High was revised and fine-tuned after evaluation of the sampling results.

RESULTS

Seismic observations and regional seismic tie to the sampling profile

The pre-Cretaceous basin structures are not very well constrained in the outer Vøring Basin and along the Vøring Transform Margin (Mìmir High). Deep-seated structural highs and deep terraces next to the Mìmir High (e.g. Rån Ridge; Zastrozhnov et al., 2020) are defined at the BCU (Base Cretaceous Unconformity) level, and were affected by Upper Jurassic - Early to mid-Cretaceous faulting (**Figs. 3** and **5**). These highs are underlain and structurally influenced by the presence of a controversial lower crustal body within the basement (Gernigon et al., 2019; Gernigon et al., 2003). Seismic data may suggest the preservation of Triassic - Jurassic successions (including local evaporites) in this outer part of the basin (Abdelmalak et al., 2017; Gernigon et al., 2003; Zastrozhnov et al., 2020). Closer to the Vøring Transform Margin, we find evidence for prominent Upper Cretaceous to late Paleocene normal faulting, except within the Mìmir High (**Fig. 5**).

In the shallowest section of the Mìmir High, the seismic data allowed us to tie and identify eight Upper Cretaceous - Cenozoic horizons ranging from the intra mid-Campanian to base Pleistocene levels (**Fig. 5**).

- The Intra Mid-Campanian horizon (IMC) correlates to the top of the Nise Formation, which has been reached by several wells in the adjacent deep Vøring Basin (e.g. Nyk High, North Gjallar Ridge). No apparent onlaps and truncations have been observed at IMC level in the proximity of the Vøring Transform Margin (**Fig. 5**). The overlying Campanian-Maastrichtian sequence is thickening towards the fault scarp of the Mímir High.
- The Base Paleogene Unconformity (BPU) represents a regional erosional surface along the flanks of the Møre and Vøring basins (Brekke, 2000; Gjelberg et al., 2005; Zastrozhnov et

al., 2020), but developed continuously from Upper Cretaceous through to early Paleocene in the central basin and main depocenters (Gjelberg et al., 2005; Zastrozhnov et al., 2020). This stratigraphic horizon is regionally well constrained and has been reached in numerous wells. We observe a slight onlap to the surface towards the fault scarp of the Mímir High. The overlying Paleocene sequence is the thickest along the fault plane in the eastern part of the Mímir High, and gradually thins towards the Vøring Transform Margin scarp.

- We interpret an Intra-Late Paleocene horizon (ILP), a marker that fits with the onset of a minor and early volcanic event, which is characterized by older vent complexes and Inner Flows within the Paleocene sequence in the outer Vøring Basin (Gernigon et al., 2015; Gernigon et al., 2019). The ILP likely corresponds to the base of a transitional zone between the Paleocene Tang and lower Eocene Tare formations (HV3 horizon of Kjoberg et al., 2017). The surface does not show any pronounced erosional features and the thickness of the overlying late (?) Paleocene strata within the Mímir High is nearly uniform.
- The Near Top Paleocene (NTP) is a regional surface that corresponds to the uppermost and youngest vent complex systems formed at the Paleocene-Eocene boundary during maximum peak volcanic activity in the Vøring Marginal High (Kjoberg et al., 2017). This horizon shows a clear erosional surface in the Mímir High with onlap and rapid thinning of overlying early Eocene strata towards the Vøring Transform Margin, and truncation on the Mìmir High.
- The Early Eocene horizon (EE) is a prominent regional surface locally displaying clear erosional features and corresponds to the top of the Tare Formation. The Tare Formation has been penetrated by many exploration wells in the outer mid-Norwegian margin (NPD factpages, 2019), but the age of the unit is somewhat debated. However, the Tare Formation is often similar in age and lithology to the Balder Formation (North Sea and

Faroe-Shetland; NPD factpages, 2019), and is therefore interpreted to be of early Eocene age (Lower Ypresian; Kjoberg et al., 2017). The EE horizon exhibits a clear onlap of the overlying Eocene strata, which rapidly thins out towards the crest of the Mímir High and another shallow structural high in the Rån Basin.

- The Near Top Eocene horizon (NTE) is another locally prominent reflection that corresponds to the internal part of the Brygge Formation. The overlying Oligocene-Miocene strata rapidly onlaps onto the NTE surface and pinches out towards the crest of the Mímir High.
- The Mid-Miocene Unconformity (MMU) is a regional erosional surface along the inverted basins formed during the middle Miocene compression (Doré et al., 2008; Eidvin et al., 2014). The MMU correlates with the base of the Kai Formation (Eidvin et al., 2014). The overlying mid-Miocene-Pliocene strata of the Kai Formation thins and pinches out towards the Mímir High.
- The Base Pleistocene (BP) is a prominent regional horizon corresponding to the base of the Naust Formation. BP marks the onset of predominantly glacial sedimentation related to the Fennoscandian Ice Sheet at the Neogene-Quaternary transition (Dahlgren et al., 2002; Ottesen et al., 2009; Rise et al., 2005). This Quaternary package within the study area represents mostly layered glacimarine sediments intercalated by mass transport deposits (Rise et al., 2010). The sequence is thinning out toward the Mímir High.

Sampling

The VTMS00 sampling profile includes 14 coring stations targeting 9 sites along the 750 m high sampling profile along the western part of the Mímir High (**Figs. 2C** and **5**). The recovery of the gravity cores ranged between 7 and 254 cm, and between 28 to 316 cm for the Selcorer. Two cores were empty (**Table 1**). Two ROV dives collected rock fragments from ten sites, with four samples from Dive#3 and six from Dive#4 (**Fig. 2C**). The results are presented on a sampling site basis and include the lithological descriptions with corresponding biostratigraphic ages.

We identified subcropping lithologies with high confidence in the bit and core catcher at seven coring stations (**Figs. 5** and **6**). They consisted of shale fragments with various levels of alteration and a green conglomerate unit. One ROV dive recovered fragments of a sill intrusion located about 300 m from the sampling profile, while we sawed off shale units from two outcrops about 1200 m from the profile. The sedimentary sequences exposed on the Mímir High fault scarp revealed ages ranging from Upper Cretaceous to early Paleocene, with an irregular thermal alteration from contact metamorphism around the sill intrusions. We also interpreted reworked Plienbachian unit in early Eocene sediments barren in in situ palynomorphs at the top of the sampling profile (sample SC2 at Site 9, **Fig. 5**).

Along the sampling profile, overburden sediments almost invariably consist of light brown to dark yellowish-brown unconsolidated clay with sand admixture. In such soft sediments, the recovery is full, unless the corer fell on its side, or hit a hard substratum preventing deeper penetration of the barrel. The overburden sediments typically contain rich, well-preserved, and very diverse marine dinoflagellate cyst assemblages that are key markers for the Pliocene to Holocene periods (Eidvin et al., 1998; Eidvin et al., 2014). In addition, the same samples also yielded a mixture of older and reworked palynomorph forms that vary in age according to the location of the sampling site along the profile (**Fig. 5**).

<u>Site 1 (sampling station SC1)</u>

Seabed sediments collected on the ocean floor at the base of the Mímir High at Site 1 (**Fig. 5**) appear to correspond to re-deposited material that was transported down slope during slumping. The material in the bit consisted of a semi-consolidated clay with numerous greenish angular, firm to soft claystone gravel and pebble size fragments giving a breccia like texture (**Fig. 6**). The reworked green clasts contained in the core material at this site are visually similar to the green conglomerate unit sampled near the top of the fault scarp at Site 8 (sampling station SC4).

Besides the Quaternary forms *Bitectatodinium tepikiense*, *Operculodinium centrocarpum*, and *Neogloboquadrina pachyderma* within the unconsolidated sediments, Site 1 contained abundant *Artemisiocysta cladodichotoma,* which are typically found in late Oligocene intervals, as well as *Homotryblium floripes* and *Cordosphaeridium cantharellum* characteristic of the late Oligocene to early Miocene intervals. The mixing of recent and Oligocene/Miocene forms of dinoflagellates most likely occurred during slumping. Since the youngest assemblages are of Pliocene to Pleistocene age, the sliding event probably occurred in the Holocene.

Site 2 (sampling stations GC1, GC2, ROV03-1, ROV03-2, ROV-03-3 and ROV03-4)

The empty core at station GC1 together with the 7 cm recovery at sampling station GC2 indicate that the substratum was probably hard enough to prevent any penetration of the core barrel. The material contained in the bit at sampling station GC2 consisted of subcrop whose lithology was lithified shale fragments enclosed in a dark yellowish-orange poorly cemented sandy matrix (**Fig. 6**).

A late Campanian age was assigned to shale fragments recovered in the bit at Site 2 (GC2). This age is based on an organic residue that almost entirely consisted of inertinitic particles, with few dark brown/grayish particles of often fragmented palynomorphs identified as *Aquilapollenites* spp., relatively common *Orbiculapollis globosus, Expressipollis* spp*.,* *Isabelidinium cooksoniae* and *Spongodinium* cf. *delitiense*. Moderately rich micropaleontology assemblages with a fair preservation were obtained. Representatives of *Bathysiphon/Rhizammina spp*. dominate, while agglutinated species like *Spiroplectammina spectabilis, Rzehakina minima*, *Saccammina placenta*, and *Saccammina complanata* are relatively rare. Contamination by Quaternary elements was also observed. Although long-ranging, these palynomorphs and micropaleontology assemblages collectively support a late Campanian age. A TAI of 4-5 in this sample (Table 1) indicates a high level of thermal maturity. Samples collected at ROV03-1 and ROV03-2 (**Fig. 7**) consist of doleritic material (Styve, 2015), which provides a simple explanation for the high thermal maturity of the organic matter observed in subcrop at site GC2 located 290 m away. Fragments of sandy siltstone were collected from outcropping strata at sites ROV-03-3 and ROV03-4 but both samples were barren in palynomorphs and could not be dated.

Site 3 (sampling station GC5)

The material in the bit at sampling station GC5 consisted of altered olive gray semi-consolidated shale intercalated with very altered and oxidized dark yellowish orange softer material (**Fig. 6**). None of the palynomorphs were in an identifiable condition, while the micropaleontology assemblages consist of moderately rich and fairly well-preserved agglutinated species like *Spiroplectammina spectabilis, Rzehakina minima, Saccammina placenta*, and *Pseudobolivina munda*, but also contained an inertinitic kerogen assemblage without any recognizable specimens. The agglutinated foraminifera indicate a Campanian to Paleocene age. However, we inferred a late Campanian to early Maastrichtian age for the Site 3 based on dating up- and down- flank, an age that supports our regional seismic interpretation (**Fig. 5**). We interpret the Paleocene forms present in the sample to be from the sediments possibly outcropping further up along the profile. The preservation state of the organic debris (TAI of 5) is very similar to that recovered from Site 2.

Site 4 (sampling stations GC3, SC3, and SC5)

Sampling station GC3 contained only soft and soupy unconsolidated sediments corresponding to overburden material, while we did not recover any sediment at the station SC3. The 40 cm recovery at station SC5 of unconsolidated soft overburden material is explained by the penetration of the core barrel being stopped by the hard and altered subcrop material recovered in the bit. At this station, the Selcorer subsequently fell on its side, resulting in an 8 kg lump of diamictite material being stuck to the outside the core barrel. Therefore, the diamictite material, which here is a heterogeneous mixture of semi-consolidated clay with pebble-size claystone and exotic crystalline dropstones that represents glacigenic deposits on the seabed.

The material in the bit at sampling station SC5 is similar in terms of lithologies and texture to the subcrop material from Site 3 and consisted of an altered olive gray semi-consolidated shale intercalated with very altered and oxidized dark yellowish orange softer clayey material. Moderately rich and well-preserved micropaleontology assemblages were identified, and included agglutinated species like *Spiroplectammina spectabilis*, *Spiroplectammina navarroana*, *Pseudobolivina munda*, *Pyrgo murrhina*, and *Eponidesum bonatus*. Contamination is observed from the overburden clay. An early Maastrichtian age was assigned to this altered material in the bit based on the few observed palynomorphs such as *Alterbidinium acutula*, and *Isabelidinium cooksoniae* (Schiøler, 1993). The TAI of 4-5 for the subcrop at Site 4 is similar to the maturity measurements at Sites 2 and 3, with inertinitic kerogen and very mature palynomorph fragments (**Table 1**).

Site 5 (sampling station GC8)

The recovery at the station GC8 includes shale fragments that have the same grey color as the enclosing sticky clay (**Fig. 6**). In this case, the sticky clay represents the alteration product of the in situ subcrop of grey shale represented by the fresh fragments. Moderately rich and moderately well-preserved agglutinating foraminifera assemblages were observed in the GC8 sample. These include species like *Spiroplectammina spectabilis*, *Haplophragmoides walteri*, *Rzehakina minima*, *Pseudobolivina munda*, *Saccammina placenta*, and *Subreophax scalaria,* which are indicators of Campanian to Paleocene ages. A late Maastrichtian age was assigned to the shale fragments in the bit based on the rich, well-preserved, and diverse marine dinoflagellate cyst assemblage where the most common forms are *Cerodinium diebelii, Phelodinium tricuspis, Laciniadinium aquiloniforme*, and *Pulchrasphaera minuscula*. The latter two forms, together with sparse *Hystrichosphaeropsis perforata*, are markers for the late Maastrichtian (Schiøler, 1993). Finally, Permian *Lueckisporites virkkiae* is found as reworked material in the GC8 sample.

Site 6 (sampling stations GC4 and GC7)

The 15 cm recovery at sampling station GC4 indicates that the substratum was hard and prevented further penetration of the core barrel. Subcrop lithology at station GC4 (**Fig. 6**) is similar to the dark yellowish angular and fragmented shale in the bit at Site 2 (station GC2). The material in the bit at the second sampling station (GC7) of Site 6 contained subcrop material consisting of brownish black semi-lithified and fragmented sandy shale (**Fig. 6**) that is overlain by overburden sediments.

Moderately rich and well-preserved micropaleontology assemblages were observed, including the agglutinated species *Spiroplectammina spectabilis* in abundance together with frequent

Pseudobolivina munda, *Rzehakina minima*, *Kalamopsis grzybowskii*, and *Saccammina placenta*. Marine dinoflagellate cysts dominate in both samples. Inertinite and wood particles are common, whereas terrestrial palynomorphs are few. Similar assemblages were met at both stations and the abundance of relatively well-preserved *Senoniasphaera inornata* together with moderate to small amounts of *Palaeoperidinium pyrophorum, Areoligera* spp., and *Spongodinium* cf. *delitiense* palynomorph assemblage suggests an earliest Paleocene age. The elevated thermal alteration (TAI of 3) at station GC7 can reflect the moderate thermal effects of a shallow level volcanic intrusion emplaced nearby. Palynomorphs known to represent the Paleocene Tang Formation are most frequent, whereas those associated with the transitional zone to the lower Eocene Tare Formation (e.g., *Apectodinium augustum*) are very rare. The latter observation is of importance, since the otherwise omnipresent *Apectodinium augustum* zone, usually very rich in its nominative species, has not been positively identified in the sampling profile. Hence, we interpret the presence of *Apectodinium augustum* at this station as a result of local contamination from the overburden. As previously mentioned, the subcrop at station GC7 is overlain by overburden sediments that are dominated by dark yellowish-brown unconsolidated clay and silts. The paleontological assemblage from this overburden package consists of a mixture of reworked *Inoceramus* prisms, other early to Upper Cretaceous palynomorph assemblages, and Pliocene to Holocene foraminifera.

<u>Site 7 (sampling station SC6)</u>

The 28 cm recovery of unconsolidated overburden sediments at sampling station SC6 indicates that the penetration of the core barrel was suddenly prevented by a hard object (subcrop or dropstone). The recovery consisted of light brown unconsolidated clay with various rounded and sub-rounded firm claystone and hard crystalline rock fragments. The core catcher material was devoid of organics, except for only a few inertinitic particles and one example of *Botryococcus* spp. The material collected at Site 7 is interpreted to represent glacigenic Pliocene to Holocene deposits including a certain amount of Eocene or older reworked sediments as represented by an agglutinated assemblage of *Spiroplectammina spectabilis* and *Bathysiphon/Rhizammina* spp.

Site 8 (sampling stations GC6 and SC4)

The age of the unconsolidated and soupy overburden clay collected at station GC6 was not determined but is assumed to be Pliocene to Holocene based on the nature of the soft sediments. The recovery at the base of SC4 consisted of a remarkable green conglomeratic unit that is overlain by one meter of unconsolidated clayey overburden sediments (**Fig. 6**). No basalt clasts were identified in this conglomerate unit. The presence of *Eatonicysta ursulae, Charlesdowniea columna*, and *Dracodinium varielongitudum*inin in the matrix are indicative of early Eocene strata (i.e. the Tare Formation). However, the abundant presence of late Paleocene markers in the pebbles such as *Alisocysta margarita, Areoligera gippingensis, Cerodinium striatum*, and *Glaphyrocysta ordinate* may provide alternative interpretation for the sediments as the Tang Formation. In addition, the matrix also contained reworked palynomorphs that are markers for the Jurassic and Cretaceous. In addition, differences in maturity from TAI and vitrinite reflectance values (**Table 1**) were measured within Upper Cretaceous and Jurassic forms, then suggesting different origins.

Site 9 (sampling station SC2)

Sampling station SC2 near the top of the Mímir High profile contained only soft and soupy unconsolidated sediments that were initially interpreted to represent only overburden yellowish-brown clays with lenses of sand. The recovery was 316 cm and can be explained by the 7-8 degrees slope that allowed accumulation of recent sediments, as well as the possible development of a full alteration profile of an underlying subcrop. Indeed, a nearly exclusively Lower Jurassic terrestrial palynomorph assemblage was identified 316 cm below the seafloor in the bit. The pollen species include *Chasmatosporites apertus, C. major, Corrolina torosus, Cerebropollenites thiergartii*, and *C. mesozoicus*. Bisaccate pollen are abundant, whereas brackish/freshwater algae *Botryococcus* spp. is regularly observed. This typical Pliensbachian-like palynomorph assemblage persists upwards in the lowermost section, but becomes increasingly diluted by younger Jurassic, Cretaceous, and in situ Quaternary overburden elements, with *Ricciisporites tuberculatus, Gonyaulacysta longicornis, Oligosphaeridium complex, Palaeocystodinium bulliforme, Nannoceratopsis gracilis,* and *Gonyaulacysta jurassica*. Pliocene to Holocene species like *Bitectatodinium tepikiense* are common 216 cm below the seafloor. The moderately rich micropaleontology assemblage, only measured in the lowermost sample of the recovery in the bit, consists of abundant planktonic and common agglutinated and calcareous benthonic Quaternary foraminifera with *Neogloboquadrina pachyderma*as as the dominating species. This unit could either be early Eocene with reworked Jurassic and barren in early Eocene species, or could instead represent Quaternary ice-rafted debris.

<u>ROV Dive#4 (ROV04-1, 2, 3, 4, 5, and 6)</u>

The sampling results from ROV Dive#4 are treated separately because the sites are located approximately 1.2 km away from the main sampling profile (Fig. 1), and thus cannot be used for direct seismic tie of line GRS99-105. Samples ROV04-1 and ROV04-4 (**Fig. 7**) gave a broad Upper Cretaceous age interpreted from an assemblage consisting of *Impagidinium* sp., *Achomosphaera* sp., *Peridinioid*, *Cerodinium diebelii*, *Kleithriasphaeridium fasciatum*, and *Leptodinium*. The two samples ROV04-2 and ROV04-3 between these Upper Cretaceous units were barren in palynomorphs and no age could be determined.

The northernmost two samples ROV04-5 and ROV04-6 (**Fig. 7**) from this dive identified a Campanian unit that is overlaid by Maastrichtian shales based on their respective palynomorph assemblages. The Campanian age is supported by the high fossil content and diversity, and dominant occurrence of *Raphidodinium fucatum*, forming a characteristic event that correlates well with the Dalsnuten (6603/5-1S) well stratigraphy at 2450 m below sea floor. The Maastrichtian age is based on the good fossil content and preservation, with key species including *Spongodinium delitiense*, *Cerodinium diebelii*, *Aquilapollenites* sp., *Palaeocystodinium australinum*, and *Chatangiella* spp. The location of the Campanian and Maastrichtian outcrops fit well with the ages determined along the GRS99-105 profile, as these two ROV sites would roughly fit between Site 2 (late Campanian), Site 3 (late Campanian – early Maastrichtian), and Site 4 (early Maastrichtian).

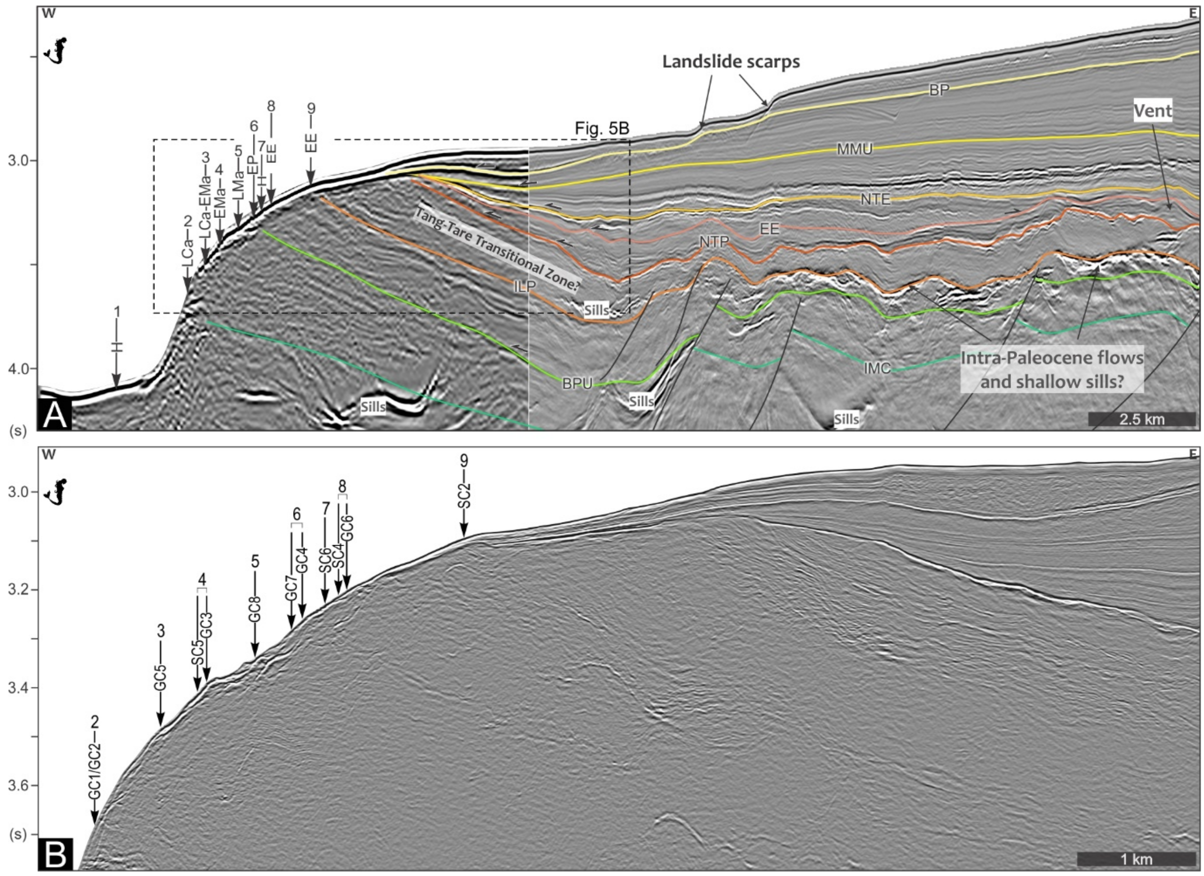

Fig. 5. A. *Zoomed part of the interpreted composite regional seismic profile (**Fig.3**) showing the Mìmir High sampling profile and sites 1 to 9, with the ages of the horizons constrained by the regional seismic interpretation and by the sampling results. IMC (Intra Mid-Campanian), BPU (Base Paleocene Unconformity), ILP (Intra-Late Paleocene), NTP (Near Top Paleocene), EE (Early Eocene), NTE (Near Top Eocene), MMU (Mid-Miocene Unconformity), BN (Base of the Naust Formation. Seismic data by courtesy of TGS.* ***B.*** *Fast track high-resolution 2D seismic line showing the location of the main sampling sites and station along the profile. Seismic data by courtesy of UiT The Arctic University of Norway.*

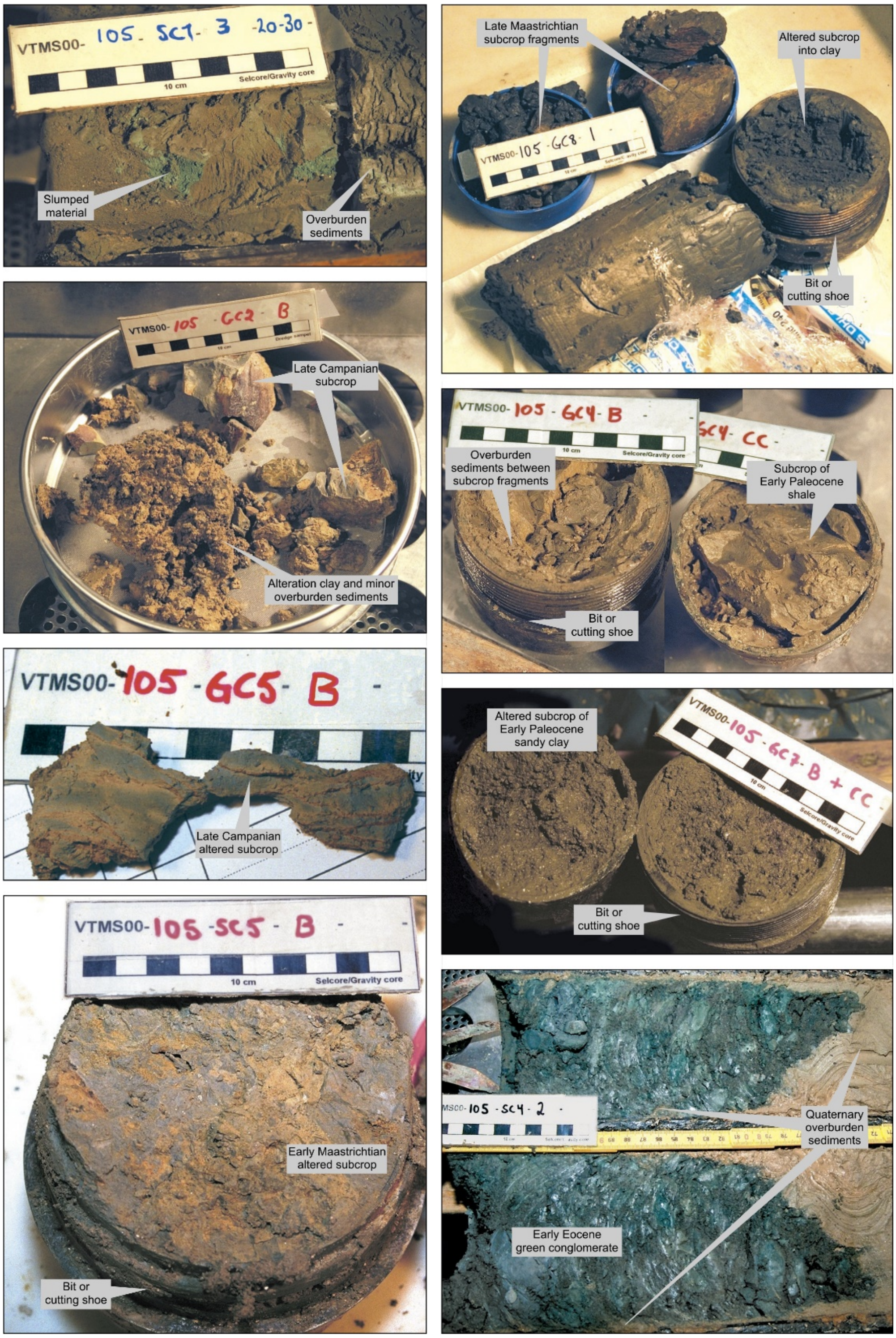

Fig. 6. *Photographs showing that the recovered material from the Mímir High varies from lithified, semi-lithified to unconsolidated clay or conglomerate (see text for details). Site names are hand-written on the scales and correspond to: VTMS00 (survey name) – 105 (profile number) – GC/SC (gravity core/Selcore) # (station number)-B/CC (bit/core catcher).*

Fig. 7. *Selected video stills from ROV dives #3 and #4 showing the nature of the seabed at the different sampling sites.*

TOC and Rock Eval Pyrolysis

The TOC and Rock Eval pyrolysis data are used to characterize the organic sediment properties of the samples and can be used to evaluate the maturation history of the area. In addition, the different populations of the vitrinite reflectance measurements may be interpreted as an indication of sediment source. For example, one population would support one source for the sediments, while several distinct populations may suggest multiple sources, each with their own maturation histories.

The analyzed samples were generally low in organic carbon (< 0.5 % TOC). Only one sample (GC7-B) had moderate to good organic carbon content with TOC concentrations above 1 % (**Table 1**). The richest samples (0.72-1.18 % TOC) were collected from sites 6, 5, and 1 (respectively GC7, GC8, and SC1). In addition to low TOC values, samples were characterized by poor quality organic matter with low S2 values (< 1 mg/g rock). Consequently, the high HI values reflect the uncertainties and unreliability of values when calculated from samples with low S2 and TOC content, but suggested types IV or III kerogen with very low hydrocarbon generation potential. Type III kerogen is mostly derived from terrestrial plants, and Type IV is characteristic of recycled or oxidized organic matter during deposition. The parameter S1 was also very low for all samples with less than 0.1 mg of free hydrocarbon per gram of rock. In addition, the production indices indicated the absence of hydrocarbon generation and migration.

Tmax values for the samples with the highest organic carbon concentration ranged from 409^{o}C to 433^{o}C (**Table 1**), which would imply immaturity. However, because of low S2 peaks measured in the same samples, the Tmax parameter, which is used to indicate maturity levels based on the maximum temperature of the S2 peak, did not deliver reliable values and little significance can be obtained considering these data alone.

The vitrinite reflectance data yielded a wide range of maturation estimates for the late Maastrichtian, Paleocene, and Eocene samples. Vitrinite reflectance values ranged from 0.38 %Ro to 1.37 %Ro, representing a spread from immature to gas/condensate generation levels. In addition, different values within the same sample suggest the presence of reworked material (**Table 1**). Sediment samples collected at Site 3 (GC5) seemed to have reached a vitrinite reflectance equivalent to oil window maturity (near peak generation) for source rocks, whereas values measured in Site 2 (GC2) samples indicated a gas/condensate level of maturity.

Station	SC1	GC1	GC2	GC5	GC3	SC3	SC5	GC8	GC4	GC7	SC6	GC6	SC4	SC2
Site	1	2	2	3	4	4	4	5	6	6	7	8	8	9
Easting (m)	447178	448706	448693	449263	449632	449626	449539	450020	450395	450299	450580	450767	450704	451707
Northing (m)	7301911	7301955	7301948	7301963	7301965	7301966	7302009	7301968	7301962	7302107	7301961	7301960	7302008	7301965
Water Depth (m)	2999	2640	2672	2538	2495	2495	2501	2465	2390	2442	2370	2352	2352	2280
Recovery (cm)	160	0	7	50	129	0	40	28	15	254	28	240	137	316
TOC (wt %)	0.95		0.25	0.05			0.32	0.72	0.24	1.18			0.25	
S1 (mg/g of rock)	0.07		0.01	0.01			0.01	0.02	0.02	0.02			0.01	
S2 (mg/g of rock)	0.87		0.02	0.10			0.05	0.20	0.09	0.38			0.07	
S3 (mg/g of rock	0.46		0.18	0.40			0.47	0.60	0.22	0.42			0.39	
HI (mg/g of TOC)	97		8	240			16	29	42	33			28	
PI (wt ratio)	0.07		0.16	0.10			0.14	0.08	0.15	0.04			0.09	
PP (mg/g of rock)	0.94		0.03	0.11			0.06	0.22	0.11	0.40			0.08	
Tmax (°C)	409		568	367			464	433	603	416			422	
Vitrinite (%Rm)			1.37	0.70				0.48	0.42	0.38			0.45	
Vitrinite (pop.2)								0.73	0.70	0.55			0.73	
Vitrinite (pop.3)								0.98	0.70	0.83			0.90	
Biostratigraphic Age	H		LCa	LCa-EMa	H?		EMa	LMa	EP	EP	H		EE	EE
TAI			4-5	5			4-5	3	3	1-3			1-2	
Lithology			Sh	Sh			Sh	Sh	Sh	Sh Sds			Sds	Clay
Reworking								Pe, K		K			P - K	EJ
Environment	DM		DM	DM			DM	SM	DM	DM	DM		SM	DM
Comments	OB		Subcrop	Subcrop	OB		Subcrop?	Subcrop	Subcrop	Subcrop	OB		Subcrop	Subcrop?

GC: gravity corer, SC: Selcorer, B: bit, CC: core catcher, TAI: thermal alteration index, Sh: shale, Sds: sandstone, SM: shallow marine, DM: deep marine
E: early, L: late, Pe: Permian, J: Jurassic, K: Cretaceous, Ca: Campanian, Ma: Maastrichtian, P: Paleocene, H: Holocene, OB: overburden sediments

Table 1. *Sampling details, Rock-Eval pyrolysis, vitrinite reflectance results, and biostratigraphy results for the samples recovered from the bit and core catcher. Coordinates given in UTM31, ED50.*

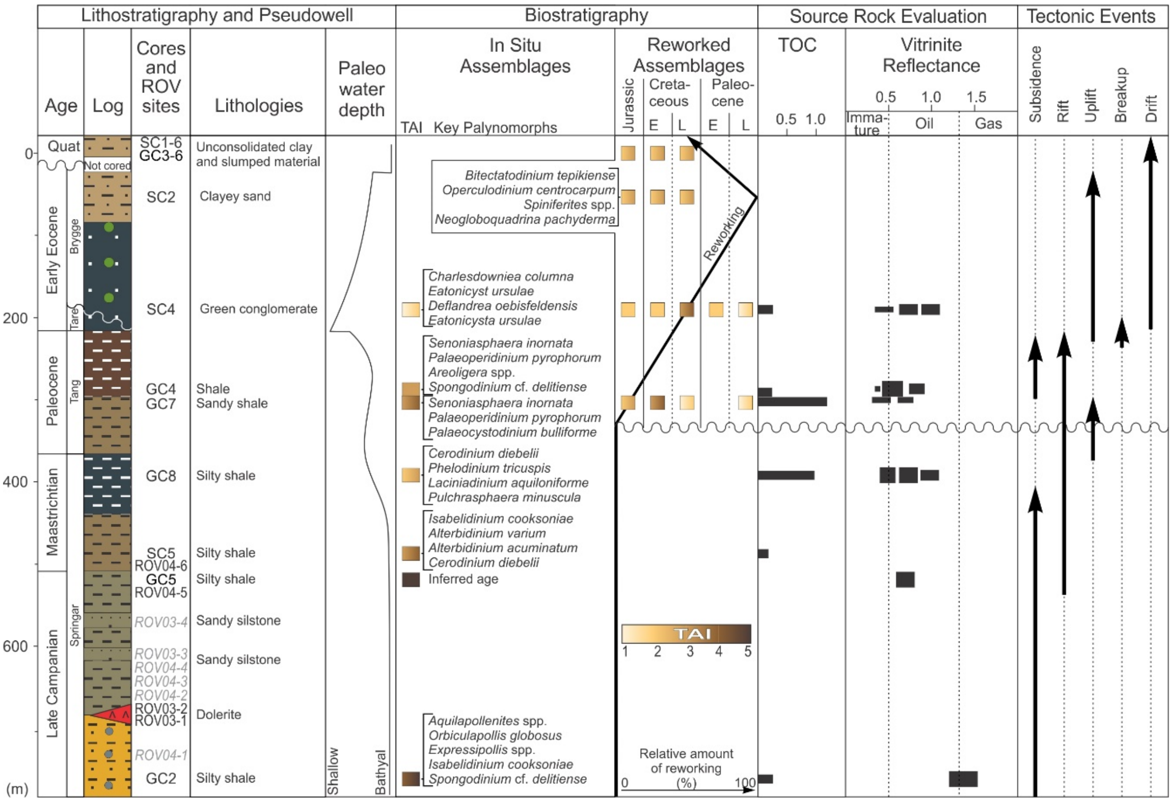

Fig. 8. *Summary figure showing the results and interpretation of the Mìmir High sampling profile. Sampling sites in grey could not be dated, and their position in the pseudowell is relative to their location along the sampling profile. The samples have been used to build the lithostratigraphic succession as pseudo-well. Paleo-water depths are interpreted from the palynomorph assemblages shown as reworked and in situ assemblages in the next columns. TOC and vitrinite reflectance data were only available for the coring samples.*

DISCUSSION

Stratigraphy of the Mìmir High

The interpretation of the semi-lithified rock fragments from the bit and core catcher (**Fig. 6**) as near *in situ* is supported by the normal sequential order of biostratigraphic ages that are younging upwards in the profile (**Table 1 and Fig. 5**), and by the Campanian and Maastrichtian ages of outcrops samples by ROV (Dive#4) about 1.2 km away from the main sampling profile. We used the results to construct a pseudo-well showing that the subcrop materials along the Mímir High sampling profile may represent a near continuous late Campanian-Eocene succession (**Fig. 8**). The basaltic rock fragments collected by the ROV Dive#3 indicate that breakup-related sills and dykes were responsible for contact metamorphism of the pre-

Eocene sequences, reflected by the elevated vitrinite reflectance and TAI measurements. The presence of *in situ* agglutinated foraminifera assemblage in the subcropping lithologies at sites 2, 3, and 4 suggests a bathyal depositional environment during the late Campanian-early Maastrichtian. The agglutinated fauna in the late Maastrichtian shales from Site 5 also indicates a bathyal environment, but the high content of terrestrial elements (pollen) and noticeable brackish/lacustrine algae may indicate a rather short distance from a vegetated coast, as well as a relative shallowing of the water depth.

The recorded palynomorph assemblage in the early Paleocene shales and clayey sandstones of Site 6 suggests that deposition took place in a deep marine environment, with reduced oxygen content near the bottom. Terrestrial palynomorphs in these sediments play a more subordinate role compared with those in the late Maastrichtian sediments of Site 5, characteristic of more open sea conditions (**Fig. 8**).

The late Paleocene interval before 55-56 Ma is well represented as pebbles in the conglomerate of Site 8, while the matrix of this conglomerate unit contains rare Jurassic, Cretaceous, abundant late Paleocene and frequent early Eocene forms. Hence, this unit is interpreted to have been deposited during the early Eocene in a shallow marine environment with the erosion and re-sedimentation of locally and newly exposed Mesozoic and late Paleocene strata.

Here, the stratigraphic results helped to constrain our seismic tie since most reflections are not well defined and neither continuous within the Mìmir High, leaving a degree of uncertainty in the interpretation. This uncertainty could also be due to the development of minor slides or slumps along the paleo-slope during the development of the Mìmir High, which are now outcropping at the seabed and visible on the high-resolution seismic line (**Fig. 5.B**). These minor slides can explain the slight misfit between the distribution of biostratigraphic ages of the samples and the ages of seismic horizons (**Fig. 5**).

Origin of Pliensbachian unit

At the top of the profile (Site 9, see **Fig. 5**) we recovered one meter of almost pure Pliensbachian pollen assemblage (e.g. *C. thiergartii* and *Botryococcus* spp.) whose upper part fades into an assemblage characteristic of recent overburden sediments. This Lower Jurassic sandy unit is strikingly similar in terms of lithology and palynomorph assemblage to the sandy Neill Klinter Formation that crops out in Jameson Land onshore East Greenland (Koppelhus and Dam, 2003). This unit is also similar to the Lower Jurassic unit (Tilje Formation?) close to the Gossa High in the Møre Basin where it is either covered by thin glacial deposits of the Naust Formation or subcrops in a relatively narrow area together with Cretaceous (Albian to Santonian) deposits (Smelror et al., 1994). The presence of Lower Jurassic sediments on top of the profile is difficult to explain at such shallow structural level because Jurassic sequences should be deeply buried in the outer mid-Norwegian margin. This unit sampled at Site 9 can either have been brought to its present location by Quaternary glacial transport, or instead by local erosion and deposition of exposed Jurassic sequences before breakup possibly in the early Eocene. The following paragraphs analyze and discuss the evidences supporting these two alternative scenarios.

Stratigraphic sampling using a gravity corer is a simple method that has been confirmed by drilling in the Baffin Bay (Abdelmalak et al., 2019). However, this approach requires to differentiate in situ from overburden material in the recovered sediment cores, which may be more difficult when the outcrop has been altered into overburden look-alike clay material or when overburden sediments are mixed with altered subcrop material (**Fig. 4**). This is the case of Site 9, where the recovered unit is interpreted to be the upper and most altered part of a subcrop alteration profile that becomes gradually mixed with the recent overburden material. Our biostratigraphic annalysis shows the same pattern that is predicted by the model (**Fig. 4**) with palynomorphs assemblages displaying an upward dilution into recent forms. Here, the Quaternary planktonic and benthonic foraminifera identified only in the bit (lowermost part of the recovery) are interpreted to be the result of contamination from the overburden during sampling. Contamination by Quaternary elements has also been identified in the subcrop lithologies at sites 2, 4, and 6. In order to explain the Pliensbachian unit, here we propose that the unit at Site 9 was reworked and redeposited locally during the early Eocene, but barren in early Eocene palynomorphs. The early Eocene age is favored since Site 9 is located above Site 8 within the profile, and this unit can only have been deposited before breakup. Although debatable, this interpretation can be tested by drilling the Mìmir High.

The alternative explanation is that the unit recovered at Site 9 represents ice rafted material during the Quaternary glaciations. The presence of early Eocene strata there does not fit with the regional seismic interpretation model of Zastrozhnov et al. (2020), and the Quaternary age would be based on the planktonic and benthonic foraminifera only identified in the bit. Glacigenic sediments consisting of diamictites were identified at Site 4 (station SC5) and the sandy clay overburden was recovered at most sites. However, none of these glacigenic deposits are as homogeneous as the one-meter-thick Lower Jurassic unit recovered at Site 9. In addition, ice rafted debris in the form of sand grains diluted in a Quaternary clay matrix (Krissek, 1989) have been identified in ODP well 642, 643, and 644 (**Fig. 2A**), but are not comparable to our meter-thick Pliensbachian unit. Another evidence not supporting a glacigenic interpretation for Site 9 is that most dropstones in the Norwegian Sea consist of high-grade metamorphic rocks, with only a small proportion of clastic sedimentary fragments where Jurassic palynormorphs are rare and only represented by Upper Jurassic (Bischof et al., 1997). Furthermore, other possible source for our potential ice rafted debris could be one of the shallow subcropped Jurassic basins in the Norwegian Shelf closer to the mainland, but the Lower Jurassic part is missing or not yet sampled (Bøe et al., 2010). Still, if the Jurassic pollen assemblage identified from the lowermost part of Site 9 were ice-rafted and sourced from the Møre Basin, a prominent mid-Cretaceous assemblage could also be expected, which is not the case for Site 9. Other possible sources for the Lower Jurassic ice rafted debris would be Traill Ø and the Jameson Land areas of Greenland (Parsons et al., 2017; Price et al., 1997; Price and Whitham, 1997; Requejo et al., 1989; Stemmerik et al., 1998) that experienced periods of significant uplift and peneplanation during the Cenozoic time (Mathiesen et al., 2000). However, Jameson Land was only covered by a thin ice cap not able to produce large amounts of erosion and icebergs able to transport Lower Jurassic sediments, except possibly during the Marine Isotope Stage 6 (MIS6 at ca. 191-130 ka BP) when the Jameson Land peninsula was overridden by the Greenland Ice Sheet (Funder et al., 2011).

Development of the Vøring Transform Margin

In this section, we summarize the development of the Mímir High and the Vøring Transform Margin based on the sampling results, seismic observations, and regional tectono-stratigraphic framework. We follow the definitions for transfer and accommodation zones of Faulds and Varga (1998) where transfer zones are discrete zones of strike-slip and oblique-slip faulting following the direction of extension, while accommodation zones are wide and diffuse transfer zones.

We suggest that during the late Campanian to early Maastrichtian the Mímir High represented a subsided accommodation zone in between overlapping active rifting zones in the outer Vøring and Møre basins and the Jan Mayen Microplate Complex (**Figs. 9** and **10**). Based on basin scale evidence, Brekke (2000) concludes that the Jan Mayen Lineament acted as a dextral transfer zone in the latest Cretaceous. Although strike-slip structures are difficult to identify on 2D seismic data, negative or positive flower structures or signs of fault reactivations were not observed in the Upper Cretaceous stratigraphic levels within the Mìmir High (**Figs. 3** and **5**). Instead, we identified domino and listric type faulting along the Gjallar Ridge and the Rån Basin (Gernigon et al., 2003; Zastrozhnov et al., 2020), thus supporting an Upper Cretaceous phase of extension in the outer Vøring Basin. At that time, the Mimir High represented a subsiding accommodation zone possibly lying in the prolongation of the Rån Basin and as part of the regional Jan Mayen Corridor (**Figs. 3, 9** and **10.A**). This accommodation zone most likely acted as an effective pathway to transport sediments from the emerged areas in the NE Greenland into the outer and distal Møre and Vøring basins as turbidite sequences (e.g., Brekke et al., 2001) similar to the well-documented Upper Cretaceous – Paleocene deep-water turbidite systems further north in the Gleipne Saddle and Surt Lineament (**Fig. 9**) (Fjellanger et al., 2005; Kjennerud and Vergara, 2005; Morton et al., 2005; Southern et al., 2017). In addition, Upper Cretaceous sediments rich in micas collected in the Southern Jan Mayen Ridge suggest limited transport most likely from Greenland (Polteau et al., 2019).

Evidence of reworked palynomorphs and increased TOC first appears in the late Maastrichtian, indicating the deposition of proximal sediments in a more restricted bathyal basin up to the early Paleocene (**Fig. 8 and 9**). The erosional character of the Base Paleogene Unconformity can be related to a regional uplift in the outer mid-Norwegian margin (Zastrozhnov et al., 2018) possibly associated with the arrival of the Iceland mantle plume (Skogseid et al., 2000). At that time, we suggest that the Vøring Transform Margin was acting as a local subsiding accommodation zone transferring sediments from the uplifted East Greenland to the outer mid-Norwegian margin (**Fig. 10.A**). Meanwhile, the adjacent Gjallar Ridge and possibly the Møre Marginal Plateau including the Jan Mayen Ridge were uplifted and locally eroded.

During the late Paleocene, the area within the Mímir High started to rise (**Fig. 10.B**). First pulses of magmatism affected the outer Møre and locally southwestern Vøring basins (Hjelstuen et al., 1999; Planke et al., 2005; Zastrozhnov et al., 2020), and the Southern Jan Mayen Ridge (Polteau et al., 2019). Steady-state seafloor spreading occurred first in between the Jan Mayen Microplate Complex and the Møre Basin around magnetic anomalies chron C24r (Thanetian-early Ypresian) but before the formation of the Inner SDR (C24n3n-C24n1n during mid-late Ypresian; Gernigon et al., 2015; Gernigon et al., 2019) and subsequent breakup phase along the Vøring Marginal High.

The chain of events suddenly accelerated with continued and rapid uplift of the Mìmir High and neighboring conjugate structures, massive volcanism, and culminated with progressive sequence of continental breakup along the entire outer mid-Norwegian margin (**Fig. 9.B**). This intense period is recoreded in the Paleocene - early Eocene, corresponding to a timespan of ca. 3-10 Ma. The rising of the Mímir High into a shallow marine environment led to the deposition of conglomerate and reworked Jurassic sediments from nearby exposed structural high containing the same exposed Jurassic sequences as on Traill Ø and Jameson Land (Parsons et al., 2017; Price et al., 1997; Price and Whitham, 1997; Requejo et al., 1989; Stemmerik et al., 1998). Late Paleocene sediments recovered on the Southern Jan Mayen Ridge (Polteau et al., 2019) are rich in reworked Upper Cretaceous marine and reworked early Paleocene terrestrial palynomorphs similar to the Egga Member (Lyck and Stemmerik, 2000), supporting the presence of exposed Mesozoic basins south of the Mímir High before breakup, possibly as tilted fault blocks. Moreover, it is tempting to speculate that the adjacent Northern Jan Mayen Ridge could represent an uplifted and eroded Jurassic block, which could be a source area for the Pliensbachian unit of Site 9 (**Fig. 10**).

Besides the early Eocene conglomerate at Site 8, possible evidence of uplift immediately before breakup is interpreted from the seismic data (**Fig. 5**) with truncation of the reflections near the top of the Mìmir High. This interpretation suggests that the Jurassic material was not ice rafted but rather transported for short distance to Site 9 within an extensive drainage system. The latter developed along the paleo-Jan Mayen Fracture Zone that fed the outer mid-Norwegian margin with material from Greenland since the Upper Cretaceous (**Fig. 9**) (Mathiesen et al., 2000). Eventually, continental separation severed this extensive drainage system, and the oceanic accretion in the Norway Basin led to the development of the oceanic transform (Jan Mayen Fracture Zone) along the Vøring Transform Margin.

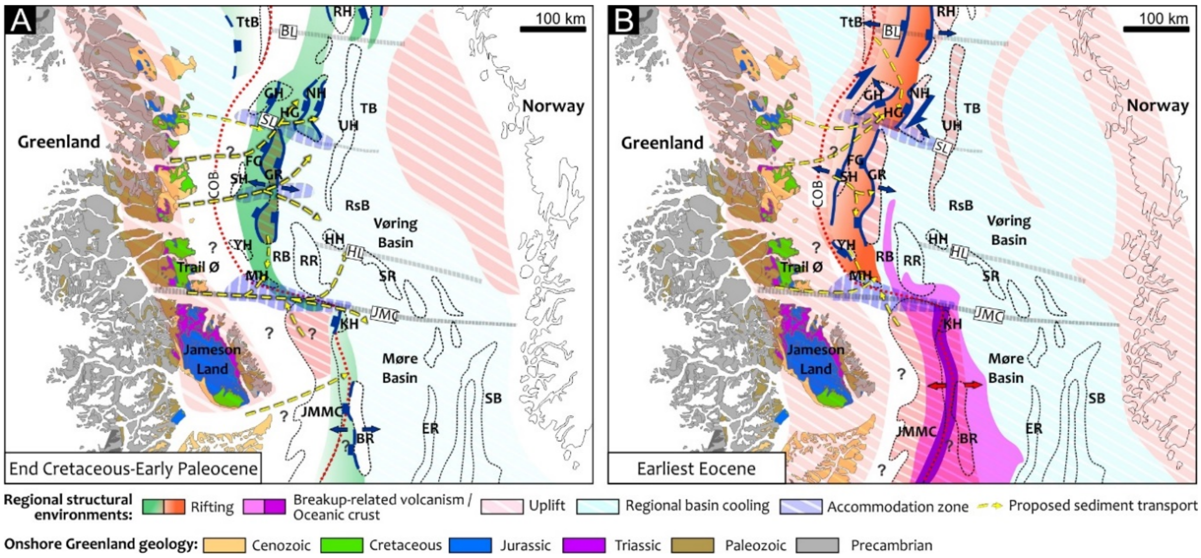

Fig. 9. *Pre-breakup paleogeographic reconstructions (modified after Zastrozhnov et al., 2020) in the end Cretaceous-early Paleocene (**A**) and end Paleocene (**B**) showing the distribution of the main drainage systems transporting eroded material from the land areas in Greenland to the mid-Norwegian margin. Onshore geology of the NE Greenland shows*

the distribution of the sedimentary sequences, which could explain the reworking patterns observed in the VTMS00 biostratigraphic studies. Onshore geology of Greenland is compiled using Harrison et al. (2011) and Escher and Pulvertaft (1995) for East Greenland. BL – Bivrost Lineament, BR – Bylgja Ridge, COB – Continent-ocean boundary, DB – Danmarkshavn Basin, ER – Ervik Ridge, FG – Fenris Graben, GH – Grimm High, GR – Gjallar Ridge, HG – Hel Graben, HH – Hevring High, HL – Hevring Lineament, JMC – Jan Mayen Corridor, JMMC – Jan Mayen Microcontinent Complex, KH - Kolga High, MH – Mímir High, NH – Nyk High, RB – Rån Basin, RH - Røst High, RR – Rån Ridge, RsB – Rås Basin, SB – Slørebotn Subbasin, SH – Skoll High, SL – Surt Lineament, SR – Slettringen Ridge, TB – Træna Basin, TtB – Thetis Basin, UH – Utgard High, YH – Ygg High.

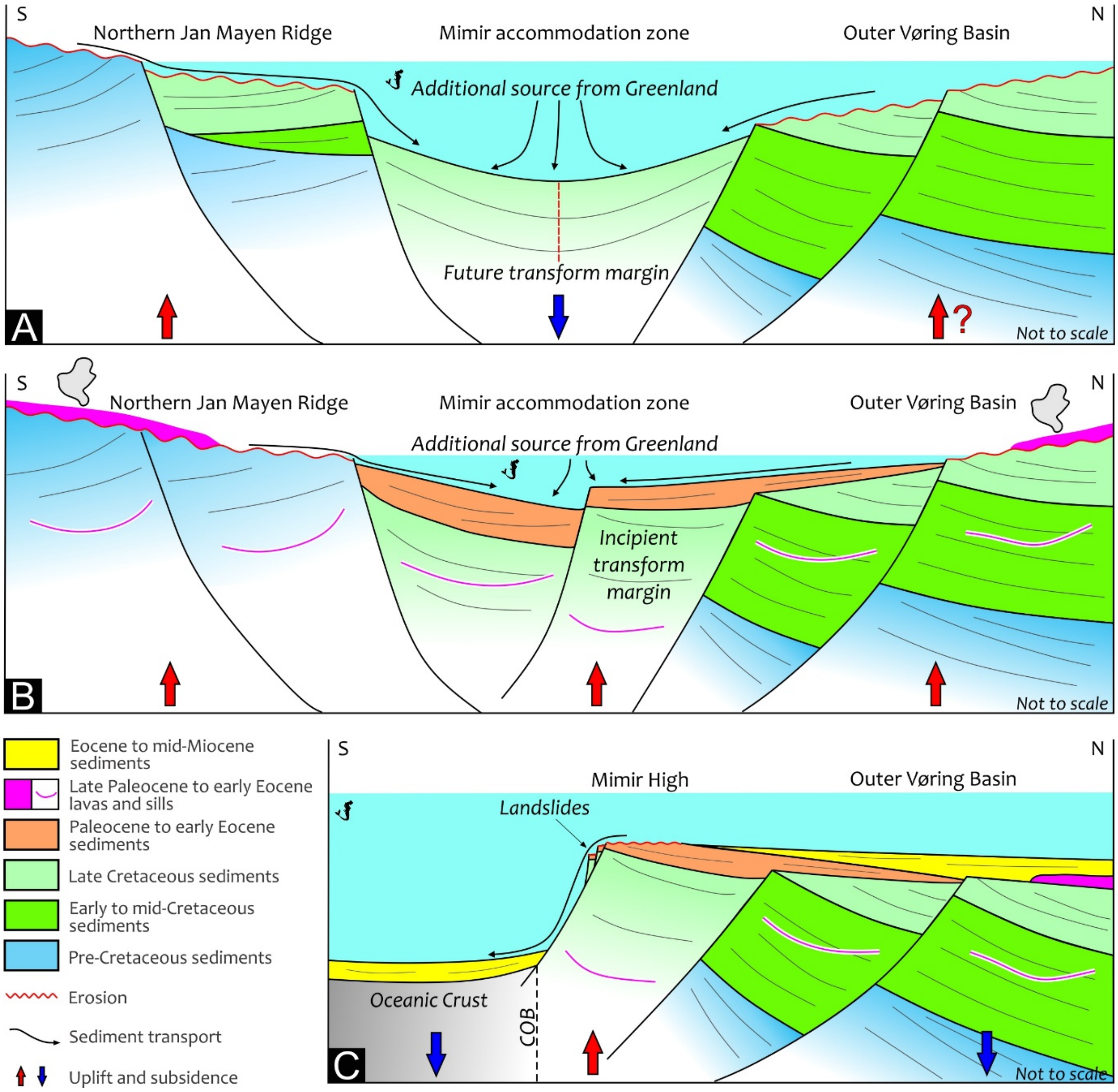

Fig. 10. *Schematic evolution of the Vøring Transform Margin at: (**A**) – Upper Cretaceous-Paleocene transition; (**B**) – Paleocene-Eocene transition; (**C**) mid-Miocene stage.*

The evolution of the Vøring Transform Margin continued during the opening of the NE Atlantic leading to the present configuration of the Mímir High. Additional younger phases of uplift and erosion occurred in the mid-Eocene, early (?) Oligocene, mid-Miocene, and Pleistocene in the Vøring and northern Møre basins (**Fig. 10.C**). The uplifted structures formed by compression (Doré et al., 2008) related to the transfer of stresses from the Jan Mayen Fracture Zone during plate reorganizations along NE Atlantic spreading systems (Gaina et al., 2009; Gernigon et al., 2012; Le Breton et al., 2012). Finally, deposition of ice-rafted debris occurred in the Vøring Transform Margin area during the Plio-Pleistocene as the result of several phases of glaciations.

CONCLUSIONS

This study shows that gravity coring is a simple and robust method to sample near in situ strata even when covered by meter-thick overburden sediments, and that ROV's are suitable for sampling exposed outcrops. The samples collected across escarpments are calibration points for tying the geology to seismic reflections, and the recovered samples can be integrated into pseudo-wells used to interpret the evolution of depositional systems in areas of limited stratigraphic control.

With respect to the stratigraphic sampling of the Mìmir High, the recovered Upper Cretaceous to early Eocene sequences recorded the pre- and syn-breakup evolution of the Vøring Transform Margin. The Mìmir High was a local subsiding depression during the Upper Cretaceous where bathyal sediments accumulated. The formation of the Vøring Transform Margin started by a rapid uplift of the Mìmir High resulting in a sudden shallowing from a Paleocene marine shale sequence into early Eocene proximal conglomerate. During the late Paleocene – early Eocene, we propose that uplifted areas on the paleo-Jan Mayen Ridge and

NE Greenland margin exposed Mesozoic sequences to weathering. At that time, the Jan Mayen Corridor probably acted as a complex accommodation zone exploited for sediment transport in an efficient drainage system bringing reworked Jurassic sediments into the outer Vøring Basin. Future acquisition of 3D seismic data combined with stratigraphic drilling (e.g. IODP project) will be crucial for imaging the geometries of structures and determining sedimentary facies and ages, which in turn could confirm our interpretation and further constrain the hydrocarbon prospectivity and geological evolution of the Vøring Transform Margin.

ACKNOWLEDGEMENTS

Many organizations and individuals have made important contributions to this report. In particular, Haavard Selnes (deceased) did the extensive offshore and onshore biostratigraphic work for the VTMS00 survey. Captain Ole Magnus Røttingen and the crew on R/V Håkon Mosby were very helpful for the sampling. We also appreciated the extensive planning and cruise work by Paul Winson, Eddie Souter, and Collin Skelton from Selantic Subsea and Professor Yngve Kristoffersen from the University of Bergen. We also thank captain Hans R. Hansen and his crew onboard R/V Helmer Hanssen of The Arctic University of Norway and all CAGE20-4 cruise participants for their excellent work during the high-resolution seismic survey in August 2020. We thank Iakov Gogin for his valuable comments on the biostratigraphy part. Sverre Planke, Dmitry Zastrozhnov, Mohamed Mansour Abdelmalak, Henrik Hovland Svensen and Adriano Mazzini acknowledge support from the Research Council of Norway through its Centres of Excellence funding scheme, project 223272. Stefan Bünz acknowledges support from the Research Council of Norway through the Centre of Excellence for Arctic Gas Hydrates, Environment and Climate (CAGE) project 223259 at UiT. Discussion and support from colleagues at TGS, from the Norwegian Petroleum Directorate, and the PL258 participants are greatly appreciated. Seismic data used in this manuscript were kindly provided by TGS. Finally, we thank the editor and reviewers for their constructive comments that improved the manuscript.

Author Contributions

Stéphane Polteau headed the manuscript writing, interpretation, and integration of the VTMS00 and ROV B2013 sampling results.

Sverre Planke, Ellen Eckhoff Planke, Henrik Svensen, Reidun Myklebust, and Bent Erland Kjølhamar participated in VTMS00 survey planning, sampling operations, and post-cruise analyses and reporting.

Dmitry Zastrozhnov, Mohamed Mansour Abdelmalak, Nina Lebedeva-Ivanova, Adriano Mazzini, and Laurent Gernigon contributed with recent seismic interpretation and tectonic models, provided the seismic-sampling tie, and participated in the interpretation of the sampling results.

Rolf Birger Pedersen and Nils Rune Sandstå participated in ROV B-2013 survey planning, sampling operations, and post-cruise analyses and reporting.

Stefan Bünz, Sverre Planke and Nina Lebedeva-Ivanova participated in the CAGE20-4 survey planning and data processing; Stefan Bünz was the cruise leader.

All authors approve the final version submitted to Marine and Petroleum Geology.

REFERENCES

Abdelmalak, M.M., Faleide, J.I., Planke, S., Gernigon, L., Zastrozhnov, D., Shephard, G.E., Myklebust, R., 2017. The T-Reflection and the deep crustal structure of the Vøring Margin offshore mid-Norway. Tectonics 36, 2017TC004617.

Abdelmalak, M.M., Meyer, R., Planke, S., Faleide, J.I., Gernigon, L., Frieling, J., Sluijs, A., Reichart, G.J., Zastrozhnov, D., Theissen-Krah, S., Said, A., Myklebust, R., 2016a. Pre-breakup magmatism on the Vøring Margin: Insight from new sub-basalt imaging and results from Ocean Drilling Program Hole 642E. Tectonophysics 675, 258-274.

Abdelmalak, M.M., Planke, S., Faleide, J.I., Jerram, D.A., Zastrozhnov, D., Eide, S., Myklebust, R., 2016b. The development of volcanic sequences at rifted margins: New insights from the structure and morphology of the Vøring Escarpment, mid-Norwegian Margin. Journal of Geophysical Resarch Solid Earth 121.

Abdelmalak, M.M., Planke, S., Polteau, S., Hartz, E.H., Faleide, J.I., Tegner, C., Jerram, D.A., Millett, J.M., Myklebust, R., 2019. Breakup volcanism and plate tectonics in the NW Atlantic. Tectonophysics.

Antobreh, A.A., Faleide, J.I., Tsikalas, F., Planke, S., 2009. Rift–shear architecture and tectonic development of the Ghana margin deduced from multichannel seismic reflection and potential field data. Marine and Petroleum Geology 26, 345-368.

Basile, C., 2015. Transform continental margins — part 1: Concepts and models. Tectonophysics 661, 1-10.

Basile, C., Allemand, P., 2002. Erosion and flexural uplift along transform faults. Geophysical Journal International 151, 646-653.

Berndt, C., Mjelde, R., Planke, S., Shimamura, H., Faleide, J.I., 2001. Controls on the tectono-magmatic evolution of a volcanic transform margin: the Vøring Transform Margin, NE-Atlantic. Marine Geophysical Researches 22, 133-152.

Berndt, C., Skogly, O.P., Planke, S., Eldholm, O., Mjelde, R., 2000. High-velocity breakup-related sills in the Vøring Basin, off Norway. J. Geophys. Res. 105, 28443-28454.

Bischof, J., Lund, J.J., Ecke, H.-H., 1997. Palynomorphs of ice rafted clastic sedimentary rocks in Late Quaternary glacial marine sediments of the Norwegian Sea as provenance indicators. Palaeogeography, Palaeoclimatology, Palaeoecology 129, 329-360.

Blystad, P., Brekke, H., Færeseth, R.B., Larsen, B.T., Skogseid, J., Tørudbakken, B., 1995. Structural elements of the Norwegian continental shelf; Part II: the Norwegian Sea Region. NPD-Bulletin 8, The Norwegian Petroleum Directorate.

Brekke, H., 2000. The tectonic evolution of the Norwegian Sea continental margin, with emphasis on the Voring and More basins, in: Nottvedt, A. (Ed.), Dynamics of the Norwegian Margin. Geological Society, pp. 327-378.

Brekke, H., Sjulstad, H.I., Magnus, C., Williams, R.W., 2001. Sedimentary environments offshore Norway— an overview, in: O.J., M., T, D. (Eds.), Sedimentary Environments Offshore Norway – Palaeozoic to Recent. NPF Special Publication, pp. 7-37.

Bøe, R., Fossen, H., Smelror, M., 2010. Mesozoic sediments and structures onshore Norway and in the coastal zone. Norges geologiske undersøkelse Bulletin 450, 15-32.

Dahlgren, K.I.T., Vorren, T.O., Laberg, J.S., 2002. Late Quaternary glacial development of the mid-Norwegian margin 65-68N. Marine and Petroleum Geology 19, 1089-1113.

Doré, A.G., Lundin, E., Kusznir, N.J., Pascal, C., 2008. Potential mechanism for the genesis of Cenozoic domal structures on the NE Atlantic margin: pros, cons and some new ideas, in: Johnson, H., Dore, A.G., Gatliff, A.G., Holdsworth, R., Lundin, E., Ritchie, J.D. (Eds.), The nature and origin of compression in passive margins. Geol. Soc. London, London, pp. 1-26.

Doré, A.G., Lundin, E.R., Jensen, L.N., Birkeland, Ø., Eliassen, P.E., Fichler, C., 1999a. Principal tectonic events in the evolution of the northwest European Atlantic margin., in: Emery, D., Myers, K. (Eds.), Sequence Stratigraphy. Blackwell Science Ltd, London.

Doré, A.G., Lundin, E.R., Jensen, L.N., Birklamd, Ø., Eliassen, P.E., Fichler, C., 1999b. Principal tectonic events in the evolution of the northwest European Atlantic margin. Geological Society, London, Petroleum Geology Conference series 5, 41-61.

Eidvin, T., Brekke, H., Riis, F., Renshaw, D.K., 1998. Cenozoic stratigraphy of the Norwegian Sea continental shelf, 64°N-68°N. Norsk Geologisk Tidsskrift 78, 125-151.

Eidvin, T., Riis, F., Rasmussen, E.S., 2014. Oligocene to Lower Pliocene deposits of the Norwegian continental shelf, Norwegian Sea, Svalbard, Denmark and their relation to the uplift of Fennoscandia: A synthesis. Marine and Petroleum Geology 56, 184-221.

Eldholm, O., Gladczenko, T.P., Skogseid, J., Planke, S., 2000. Atlantic volcanic margins: a comparative study, in: NOTTVEDT, A.e.a. (Ed.), Dynamics of the Norwegian Margin. Geological Society, London. Spetial Publications, London, pp. 411-428.

Eldholm, O., Grue, K., 1994. North Atlantic volcanic margins: Dimensions and production rates. Journal of Geophysical Research 99, 2955-2968.

Espitalié, J., Deroo, G., Marquis, F., 1986. La pyrolyse Rock-Eval et ses applications, Part III. Revue Institut Français de Pétrole 41, 467-481.

Faleide, J.I., Myhre, A.M., O., E., 1988. Early Tertiary volcanism at the western Barents Sea margin, in: Morton, A., Parson, L.M. (Eds.), Early Tertiary Volcanism and the Opening of the NE Atlantic. Geol. Soc. Special Publ., pp. 135-146.

Faleide, J.I., Tsikalas, F., Breivik, A.J., Mjelde, R., Ritzmann, O., Engen, Ø., Wilson, J., Eldholm, O., 2008. Structure and evolution of the continental margin off Norway and the Barents Sea. Episodes 31, 82-91.

Faulds, J.E., Varga, R.J., Faulds, J.E., Stewart, J.H., 1998. The role of accommodation zones and transfer zones in the regional segmentation of extended terranes, Accommodation zones and transfer zones; the regional segmentation of the Basin and Range Province. Geological Society of America, p. 0.

Fjellanger, E., Surlyk, F., Wamsteeker, L.C., Midtun, T., 2005. Upper Cretaceous basin-floor fans in the Vøring Basin, Mid Norway shelf, in: Wandås, B., Nystuen, T.G.J.P., Eide, E.A., Gradstein, F.M. (Eds.), Onshore-Offshore Relationships on the North Atlantic Margin. Elsevier, Amsterdam, pp. 135-164.

Funder, S., Kjeldsen, K.K., Kjær, K.H., Ó Cofaigh, C., 2011. Chapter 50 - The Greenland Ice Sheet During the Past 300,000 Years: A Review, in: Ehlers, J., Gibbard, P.L., Hughes, P.D. (Eds.), Developments in Quaternary Sciences. Elsevier, pp. 699-713.

Gaina, C., Gernigon, L., Ball, P., 2009. Palaeocene-Recent plate boundaries in the NE Atlantic and the formation of the Jan Mayen microcontinent. Journal of the Geological Society 166, 601-616.

Ganerød, M., Smethurst, M.A., Torsvik, T.H., Prestvik, T., Rousse, S., McKenna, C., Van Hinsbergen, D.J.J., Hendriks, B.W.H., 2010. The North Atlantic Igneous Province reconstructed and its relation to the Plume Generation Zone: the Antrim Lava Group revisited. Geophysical Journal International 182, 183-202.

Gernigon, L., Blischke, A., Nasuti, A., Sand, M., 2015. Conjugate volcanic rifted margins, seafloor spreading, and microcontinent: Insights from new high-resolution aeromagnetic surveys in the Norway Basin. Tectonics 34, 907-933.

Gernigon, L., Franke, D., Geoffroy, L., Schiffer, C., Foulger, G.R., Stoker, M., 2019. Crustal fragmentation, magmatism, and the diachronous opening of the Norwegian-Greenland Sea. Earth-Science Reviews.

Gernigon, L., Gaina, C., Olesen, O., Ball, P.J., Péron-Pinvidic, G., Yamasaki, T., 2012. The Norway Basin revisited: From continental breakup to spreading ridge extinction. Marine and Petroleum Geology 35, 1-19.

Gernigon, L., Ringenbach, J.-C., Planke, S., Le Gall, B., 2004. Deep structures and breakup along volcanic rifted margins: insights from integrated studies along the outer Vøring Basin (Norway). Marine and Petroleum Geology 21, 363-372.

Gernigon, L., Ringenbach, J.C., Planke, S., Gall, B.L., Jonquet-KolstO, H., 2003. Extension, crustal structure and magmatism at the outer Voring Basin, Norwegian margin. Journal of the Geological Society 160, 197-208.

Gjelberg, J., Martinsen, O.J., Charnok, M., Møller, N., Antonsen, P., 2005. The Late Maastrichtian–Early Paleocene Ormen Lange gas field., in: Doré, A.G., Vining, B.A. (Eds.), Petroleum Geology: North-West Europe and Global Perspectives - Proceedings of the 6th Petroleum Geology Conference. Geological Society, London, pp. 1165–1184.

Hansen, J., Jerram, D.A., McCaffrey, K., Passey, S.R., 2009. The onset of the North Atlantic Igneous Province in a rifting perspective. Geological Magazine 146, 309-325.

Hjelstuen, B.O., Eldholm, O., Skogseid, J., 1999. Cenozoic evolution of the northern Voring margin. Bulletin of the Geological Society of America 111, 1792-1807.

Kjennerud, T., Vergara, L., 2005. Cretaceous to Palaeogene 3D palaeobathymetry and sedimentation in the Vøring Basin, Norwegian Sea. Geological Society, London, Petroleum Geology Conference series 6, 815.

Kjoberg, S., Schmiedel, T., Planke, S., Svensen, H.H., Millett, J.M., Jerram, D.A., Helsem, A., 2017. 3D structure and formation of hydrothermal vent complexes at the Paleocene-Eocene transition, the Møre Basin, mid-Norwegian margin. Interpretations 5, SK65-SK81.

Koppelhus, E.B., Dam, G., 2003. Palynostratigraphy and palaeoenvironments of the Rævekløft, Gule Horn and Ostreaelv Formations (Lower–Middle Jurassic), Neill Klinter Group, Jameson Land, East Greenland. Geological Survey of Denmark and Greenland Bulletin 1, 723-775.

Krissek, L.A., 1989. 4. Late Cenozoic records of ice-rafting at ODP sites 642, 643, and 644, Norwegian Sea: Onset, chronology, and characteristics of glacial/interglacial fluctuations., in: Eelholm, O., Thiede, J., S, Taylor, E., al., e. (Eds.), Proceedings of the Ocean Drilling Program, Scientific Res, pp. 61-74.

Kristoffersen, Y., Lien, E., Festervoll, K., Ree, S., Åardahl, K., Hosøy, Ø., 2006. The hydrostatic corer Selcore—a tool for sediment sampling and geophysical site characterization. Marine Geology 229, 101-112.

Kvarven, T., Mjelde, R., Hjelstuen, B.O., Faleide, J.I., Thybo, H., Flueh, E.R., Murai, Y., 2016. Crustal composition of the Møre Margin and compilation of a conjugate Atlantic margin transect. Tectonophysics 666, 144-157.

Lafarge, E., Marquis, F., Poillot, D., 1998. Rock-Eval 6 application in hydrocarbon exploration, production, and soil contamination studies. Revue Institut Français de Pétrole 56 (4), 421-437.

Le Breton, E., Cobbold, P.R., Dauteuil, O., Lewis, G., 2012. Variations in amount and direction of seafloor spreading along the northeast Atlantic Ocean and resulting deformation of the continental margin of northwest Europe. Tectonics 31.

Lien, T., Midtbø, R.E., Martinsen, O.J., 2006. Depositional facies and reservoir quality of deep-marine sandstones in the Norwegian Sea. Norwegian Journal of Geology 86, 71-92.

Loncke, L., Maillard, A., 2015. Structure of the Demerara passive transformmargin and associated sedimentary processes., in: Nemčok, M., Rybár, S., Sinha, S.T., Hermeston, S.A. (Eds.), TransformMargins: Development, Controls and Petroleum Systems. Geological Society, Special Publications, London, p. 431.

Loncke, L., Roest, W.R., Klingelhoefer, F., Basile, C., Graindorge, D., Heuret, A., Marcaillou, B., Museur, T., Fanget, A.S., Mercier de Lépinay, M., 2020. Transform Marginal Plateaus. Earth-Science Reviews 203, 102940.

Lorenzo, J.M., Mutter, J.C., Larson, R.L., 1991. Development of the continent-ocean transform boundary of the southern Exmouth Plateau. Geology 19, 843-846.

Lorenzo, J.M., Vera, E.E., 1992. Thermal uplift and erosion across the continent-ocean transform boundary of the southern Exmouth Plateau. Earth and Planetary Science Letters 108, 79-92.

Lundin, E.R., Doré, A.G., 1997. A tectonic model for the Norwegian passive margin with implications for the NE Atlantic: Early Cretaceous to break-up. Journal of the Geological Society 154, 545-550.

Lyck, J.M., Stemmerik, L., 2000. Palynology and depositional history of the Paleocene? Thyra Ø Formation, Wandel Sea Basin, eastern North Greenland. Geology of Greenland Survey Bulletin 187, 21-49.

Mascle, J., Lohmann, G.P., Moullade, M., 1998. Proceedings ODP, Scientific Results, in: Mascle, J., Lohmann, G.P., Moullade, M. (Eds.). Ocean Drilling Program, College Station, TX.

Mathiesen, A., Bidstrup, T., Christiansen, F.G., 2000. Denudation and uplift history of the Jameson Land basin, East Greenland--constrained from maturity and apatite fission track data. Global and Planetary Change 24, 275-301.

Mercier de Lépinay, M., Loncke, L., Basile, C., Roest, W.R., Patriat, M., Maillard, A., De Clarens, P., 2016. Transform continental margins – Part 2: A worldwide review. Tectonophysics 693, 96-115.

Meyer, R., van Wijk, J., Gernigon, L., 2007. The North Atlantic Igneous Province: A review of models for its formation. Geological Society of America Special Papers 430, 525-552.

Mjelde, R., Breivik, A.J., Raum, T., Mittelstaedt, E., Ito, G., Faleide, J.I., 2008. Magmatic and tectonic evolution of the North Atlantic. Journal of the Geological Society 165, 31-42.

Mjelde, R., Faleide, J.I., Breivik, A.J., Raum, T., 2009. Lower crustal composition and crustal lineaments on the Vøring Margin, NE Atlantic: A review. Tectonophysics 472, 183-193.

Mjelde, R., Raum, T.A.B., Shimamura, H., Murai, Y., Takanami, T., Faleide, J.I., 2005. Crustal structure of the Vøring margin, NE Atlantic: a review of geological implications based on recent OBS-data., in: Doré, A.G., Vining, B.A. (Eds.), North-West European Petroleum Geology and Global Perspectives: Proceedings of the 6th Conference. Geological Society of London,, pp. 803-813.

Morton, A.C., Whitham, A.G., Fanning, C.M., Claoué-Long, J., Bjørn T.G Wandås, J.P.N.E.E., Felix, G., 2005. The role of East Greenland as a source of sediment to the Vøring Basin during the Late Cretaceous, Norwegian Petroleum Society Special Publications. Elsevier, pp. 83-110.

Nemčok, M., Rybár, S., Sinha, S.T., Hermeston, S.A., Ledvényiová, L., 2016. Transform margins: development, controls and petroleum systems – an introduction. Geological Society, London, Special Publications 431, 1-38.

Ottesen, D., Rise, L., Andersen, E.S., Bugge, T., Eidvin, T., 2009. Geological evolution of the Norwegian continental shelf between 61N and 68N during the last 3 million years. . Norwegian Journal of Geology 89, 251-265.

Parsons, A.J., Whitham, A.G., Kelly, S.R.A., Vautravers, B.P.H., Dalton, T.J.S., Andrews, S.D., Pickles, C.S., Strogen, D.P., Braham, W., Jolley, D.W., Gregory, F.J., 2017. Structural evolution and basin architecture of the Traill Ø region, NE Greenland: A record of polyphase rifting of the East Greenland continental margin. Geosphere 13, 733-770.

Pattier, F., Loncke, L., Gaullier, V., Basile, C., Maillard, A., Imbert, P., Roest, W., Vendeville, B., Patriat, M., Loubrieu, B., 2013. Mass-transport deposits and fluid venting in a transform margin setting, the eastern Demerara Plateau (French Guiana). Marine & Petroleum Geology 46, 287-303.

Péron-Pinvidic, G., Osmundsen, P.T., 2016. Architecture of the distal and outer domains of the Mid-Norwegian rifted margin: Insights from the Rån-Gjallar ridges system. Marine and Petroleum Geology 77, 280-299.

Planke, S., Rasmussen, T., Rey, T., Myklebust, R., 2005. Seismic characteristics and distribution of volcanic intrusions and hydrothermal vent complexes in the Vøring and Møre basins, in: Doré, A.G., and Vining, B. A., (Ed.), Petroleum Geology: North-West Europe and Global Perspectives-Proceedings of the 6th Petroleum Geology Conference. Geological Society, London, pp. 833–844.

Polteau, S., Mazzini, A., Hansen, G., Planke, S., Jerram, D.A., Millett, J., Abdelmalak, M.M., Blischke, A., Myklebust, R., 2019. The pre-breakup stratigraphy and petroleum system of the Southern Jan Mayen Ridge revealed by seafloor sampling. Tectonophysics 760, 152-164.

Price, S., Brodie, J., Whitham, A., Kent, R., 1997. Mid-Tertiary rifting and magmatism on the Traill O Region, East Greenland. Journal of the Geological Society, London 154, 419-434.

Price, S.P., Whitham, A.G., 1997. Exhumed hydrocarbon traps in East Greenland; analogs for the Lower-Middle Jurassic play of Northwest Europe. AAPG Bulletin 81, 196-221.

Raum, T., Mjelde, R., Digranes, P., Shimamura, H., Shiobara, H., Kodaira, S., Haatvedt, G., Sørenes, N., Thorbjørnsen, T., 2002. Crustal structure of the southern part of the Vøring Basin, mid-Norway margin, from wide-angle seismic and gravity data. Tectonophysics 355, 99-126.

Requejo, A.G., Hollywood, J., Halpern, H.I., 1989. Recognition and Source Correlation of Migrated Hydrocarbons in Upper Jurassic Hareelv Formation, Jameson Land, East Greenland. AAPG Bulletin 73, 1065-1088.

Rise, L., Chand, S., Hjelstuen, B.O., Haflidason, H., Bøe, R., 2010. Late Cenozoic geological development of the south Vøring margin, mid-Norway. Marine and Petroleum Geology 27, 1789-1803.

Rise, L., Ottesen, D., Berg, K., Lundin, E., 2005. Large-scale development of the midNorwegian margin during the last 3 million years. . Marine and Petroleum Geology 22, 33-44.

Saunders, A.D., Fitton, J.G., Kerr, A.C., Norry, M.J., Kent, R.W., 1997. The North Atlantic igneous province, in: Mahoney, J.J., Coffin, M.F. (Eds.), Large Igneous Provinces: Continental, Oceanic, and Planetary Flood Volcanism. AGU Geophysical Monograph, Washington, pp. 45-93.

Schiøler, P., 1993. New species of dinoflagellate cysts from Maastrichtian – Danian chalks of the Danish North Sea. Journal of Micropalaeontolgy 12, 99-112.

Skogseid, J., Eldholm, O., 1987. Early Cenozoic Crust at the Norwegian Continental Margin and the Conjugate Jan Mayen Ridge. J. Geophys. Res. 92(B11), 11471-11491.

Skogseid, J., Planke, S., Faleide, J.I., Pedersen, T., Eldholm, O., Neverdal, F., 2000. NE Atlantic continental rifting and volcanic margin formation. Geological Society, London, Special Publications 167, 295-326.

Smelror, M., Jacobsen, T., Rise, L., Skarbø, O., Verdenius, J.G., Vigran, J.O., 1994. Jurassic to Cretaceous stratigraphy of shallowcores on the Møre basin margin, Mid-Norway. Norsk Geologisk Tidsskrift 74, 89-107.

Southern, S.J., Kane, I.A., Warchoł, M.J., Porten, K.W., McCaffrey, W.D., 2017. Hybrid event beds dominated by transitional-flow facies: character, distribution and significance in the Maastrichtian Springar Formation, north-west Vøring Basin, Norwegian Sea. Sedimentology 64, 747-776.

Stemmerik, L., Dam, G., Noe-Nygaard, N., Piasecki, S., Surluk, F., 1998. Sequence stratigraphy of source and reservoir rocks in the Upper Permian and Jurassic of Jameson Land, East Greenland. Geol. Soc. Greenland Survey Bull. 180, 43-54.

Styve, E., 2015. Petrogenesis of igneous samples from the Gjallar Ridge and the Vøring Spur, Department of Earth Science. University of Bergen, Bergen, p. 161.

Talwani, M., Eldholm, O., 1977. Evolution of the Norwegian Greenland Sea. Geological Society of America Bulletin 88, 969-999.

Torsvik, T.H., Mosar, J., Eide, E.A., 2001. Creataceous-Tertiary geodynamics: A North Atlantic exercise. Geophysical Journal International 146, 850-866.

Tsikalas, F., Faleide, J.I., Eldholm, O., Antonio Blaich, O., 2012. 5 - The NE Atlantic conjugate margins, in: Roberts, D.G., Bally, A.W. (Eds.), Regional Geology and Tectonics: Phanerozoic Passive Margins, Cratonic Basins and Global Tectonic Maps. Elsevier, Boston, pp. 140-201.

Tsikalas, F., Faleide, J.I., Kuznir, N.J., 2008. Along-strike variations in rifted margin crustal architecture and lithosphere thinning between northern Vøring and Lofoten margin segments off mid-Norway. tectonophysics 458, 68-81.

Turner, J.P., Rosendahl, B.R., Wilson, P.G., 2003. Structure and evolution of an obliquely sheared continental margin: Rio Muni, West Africa. Tectonophysics 374, 41-55.

Weiss, H.M., Wilhelms, A., Mills, N., Scotchmer, J., Hall, P.B., Lind, K., Brekke, T., 2000. NIGOGA- The Norwegian Industry Guide to organic Geochemical Analyses (online). Available from World Wide Web: htttp://www.npd.no/engelsk/nigoga/default.htm. Norsk Hydro, Statoil, Geolab Nor, SINTEF Petroleum Research and the Norwegian Petroleum Directorate, p. 102.

Zastrozhnov, D., Gernigon, L., Gogin, I., Abdelmalak, M.M., Planke, S., Faleide, J.I., Eide, S., Myklebust, R., 2018. Cretaceous-Paleocene Evolution and Crustal Structure of the Northern Vøring Margin (Offshore Mid-Norway): Results from Integrated Geological and Geophysical Study. Tectonics 37, 497-528.

Zastrozhnov, D., Gernigon, L., Gogin, I., Planke, S., Abdelmalak, M.M., Polteau, S., Faleide, J.I., Manton, B., Myklebust, R., 2020. Regional structure and polyphased Cretaceous-Paleocene rift and basin development of the mid-Norwegian volcanic passive margin. Marine and Petroleum Geology 115.

Ziegler, P.A., 1988. Evolution of the Arctic-North Atlantic and the Western Tethys. American Association of Petroleum Geologist Memoir 43.